Discrete immune response signature to SARS-CoV-2 mRNA vaccination versus infection

Ellie N. Ivanova[1*], Joseph C. Devlin[2,3*], Terkild B. Buus[1,4*], Akiko Koide[6,8], Amber Cornelius[5], Marie I. Samanovic[5,6], Alberto Herrera[1], Chenzhen Zhang[3], Ludovic Desvignes[5,9], Niels Odum[4], Robert Ulrich[5], Mark J. Mulligan[5], Shohei Koide[8,10], Kelly V. Ruggles[2], Ramin S. Herati[5,6#], Sergei B. Koralov[1#]

[1] Department of Pathology, NYU Grossman School of Medicine, New York, NY, 10016, USA.

[2] Institute of Systems Genetics, New York University Grossman School of Medicine, New York, NY 10016, USA

[3] Vilcek Institute of Graduate Biomedical Sciences, New York University Grossman School of Medicine, New York, NY 10016, USA.

[4] LEO Foundation Skin Immunology Research Center, Department of Immunology and Microbiology, University of Copenhagen, DK-2200 Copenhagen, Denmark

[5] New York University Langone Vaccine Center and New York University Grossman School of Medicine, New York, NY, 10016, USA.

[6] Department of Medicine, NYU Grossman School of Medicine, New York, NY, 10016, USA

[7] Department of Microbiology, NYU Grossman School of Medicine, 430 East 29th Street, New York, NY, 10016, USA.

[8] Perlmutter Cancer Center, NYU Langone Health, New York, NY, 10016, USA.

[9] Office of Science and Research, NYU Langone Health, New York, NY, 10016, USA.

[10] Department of Biochemistry and Molecular Pharmacology, New York University Grossman School of Medicine, New York, NY 10016, USA.

*Contributed equally to this work

#Address correspondence: sergei.koralov@nyulangone.org and ramin.herati@nyulangone.org

Abstract

Both SARS-CoV-2 infection and vaccination elicit potent immune responses. A number of studies have described immune responses to SARS-CoV-2 infection. However, beyond antibody production, immune responses to COVID-19 vaccines remain largely uncharacterized. Here, we performed multimodal single-cell sequencing on peripheral blood of patients with acute COVID-19 and healthy volunteers before and after receiving the SARS-CoV-2 BNT162b2 mRNA vaccine to compare the immune responses elicited by the virus and by this vaccine. Phenotypic and transcriptional profiling of immune cells, coupled with reconstruction of the B and T cell antigen receptor rearrangement of individual lymphocytes, enabled us to characterize and compare the host responses to the virus and to defined viral antigens. While both infection and vaccination induced robust innate and adaptive immune responses, our analysis revealed significant qualitative differences between the two types of immune challenges. In COVID-19 patients, immune responses were characterized by a highly augmented interferon response which was largely absent in vaccine recipients. Increased interferon signaling likely contributed to the observed dramatic upregulation of cytotoxic genes in the peripheral T cells and innate-like lymphocytes in patients but not in immunized subjects. Analysis of B and T cell receptor repertoires revealed that while the majority of clonal B and T cells in COVID-19 patients were effector cells, in vaccine recipients clonally expanded cells were primarily circulating memory cells. Importantly, the divergence in immune subsets engaged, the transcriptional differences in key immune populations, and the differences in maturation of adaptive immune cells revealed by our analysis have far-ranging implications for immunity to this novel pathogen.

Introduction

In 2019, a novel coronavirus (SARS-CoV-2) emerged and the resulting pandemic has had unprecedented impact on the heath, economy, and social fabric of the global community. The clinical presentation of coronavirus disease 2019 (COVID-19), the disease caused by SARS-CoV-2, has been highly heterogeneous, with manifestations ranging from asymptomatic or mild illness, to acute respiratory distress syndrome (ARDS), multiorgan failure, and death. In the past year, there have been over 141 million confirmed infections and 3 million deaths worldwide[1].

To date, a number of comprehensive studies have described immune responses to SARS-CoV-2 infection[2-7]. These research efforts identified lymphopenia with concomitant innate cell expansion, while specific alterations in a number of immune subsets, including activated CD8 T cells, plasma cells, monocytes, and NK cells, are thought to shape the clinical outcomes of patients. Immune responses in individuals who survive COVID-19 eventually return to baseline, with establishment of memory T and B cell responses[8-11], and corresponding development of a neutralizing antibody repertoire[12,13]. Although memory responses to COVID-19 are evident in convalescent individuals, the longevity of immune memory to SARS-CoV-2 and molecular and cellular characteristics responsible for durability of these responses remain to be elucidated.

Infection with SARS-CoV-2 and vaccination against the virus have both been shown to stimulate immune responses and protect against subsequent infection[14-20]. SARS-CoV-2 contains four structural proteins, the envelope (E) and membrane (M) proteins, which insert into the viral

envelope, the nucleocapsid (NC) protein, which binds the viral RNA, and the spike (S) glycoprotein, another viral envelope protein which binds to receptors on the host cell via the receptor-binding domain (RBD)[21,22]. In contrast, the BNT162b2 mRNA vaccine contains a lipid nanoparticle-formulated nucleoside-modified mRNA that encodes the prefusion stabilized form of the S protein only[23-25]. Both infection and vaccination generate protective anti-S memory immune responses[14-16]. However, the innate and adaptive immunity established by each is likely to be substantially qualitatively different from the other. Comparison of immune responses generated by the vaccine and the virus provides a unique opportunity to juxtapose antigen driven response to the profound inflammatory response associated with infection.

In our study, we took advantage of 5'-CITE-seq (5' Cellular Indexing of Transcriptomes and Epitopes by sequencing), a multimodal, single-cell sequencing technique, to simultaneously characterize the surface protein phenotype and transcriptome of immune cells[26,27]. This platform also enables reconstruction of B cell and T cell antigen receptor rearrangement of individual lymphocytes. We utilized the 5'-CITE-seq platform to characterize cellular and transcriptional responses to SARS-CoV-2 infection and vaccination in peripheral immune cells in an effort to better understand the host response to the pathogen and immunization against defined viral antigens. We also used a recently developed multiplex bead-binding assay to quantify virus-specific antibody titers in the serum of COVID-19 patients and vaccine recipients.

Our multimodal analysis revealed dramatic alterations in the frequencies and transcriptional programs of many immune subsets in response to infection and highlighted differences in the breadth of immune response observed upon infection and vaccination. In COVID-19 patients, transcriptional profiles of many immune populations were characterized by augmented interferon (IFN) signaling, upregulation of genes associated with cytotoxicity, and changes in metabolic pathways. Analysis of peripheral immune cells following vaccination with the SARS-CoV-2 BNT162b2 mRNA vaccine revealed alterations of transcriptional programs of several immune populations consistent with immune activation, but the highly augmented IFN signaling and cytotoxic signature observed in COVID-19 patients were largely absent. We observed robust antibody response in both COVID-19 patients and immunized individuals, with vaccination inducing a remarkably consistent IgG and IgA response to S protein. Interestingly, the nature of clonal B and T cell responses differed dramatically between infected and vaccinated individuals, suggesting that inflammatory responses associated with infection influence the trajectory of the adaptive immune response. While both infection and vaccination elicit vigorous immune responses, the difference in the nature of immune populations engaged and in maturation of adaptive immune responses is likely to impact the durability of protective immunity.

Results

Overview of immune responses to COVID-19 infection and immunization

Better understanding of immune responses to SARS-CoV-2 antigens in different inflammatory contexts will lead to improved therapeutics and more robust vaccines. To accomplish this, we profiled circulating immune cells from five adults with acute COVID-19 and five healthy adults, three of whom received the SARS-CoV-2 BNT162b2 mRNA vaccine, and two who were SARS-CoV-2 naïve. Samples were taken at multiple time points resulting in a total of 30 samples (**Schematic 1**). Three individuals were sampled during the acute phase of infection and two in later stage of disease, with longitudinal samples collected from four of the five patients. Time points were recorded as days post-onset (DPO) of symptoms, and clinical metadata were evaluated for clinical severity based on the WHO clinical progression scale[28]. All subjects in the vaccine group received two doses of the vaccine approximately three weeks apart, in accordance with its FDA Emergency Use Authorization. For vaccine responses, samples were collected at baseline, and then at approximately 1, 2, 3, 4, 5, and 7 weeks after the first vaccine dose. For all participants, demographic characteristics, clinical features, and outcomes are listed in **Supplemental Table 1**.

To assess the impact of SARS-CoV-2 infection and vaccination on the individuals' global immune landscape, we leveraged multimodal 5'-CITE-seq approach[26] to identify discrete clusters based on transcriptional profile and surface phenotype of circulating cells. To do this, peripheral blood mononuclear cells (PBMCs) were multiplexed and sequenced using 5' droplet-based scRNA-seq technology (10x Genomics). Surface marker phenotypes were detected using an optimized 60 antibody CITE-seq panel[29], generating matching transcriptional and surface protein data. In addition, single-cell T cell receptor (TCR) αβ and γδ, as well as B cell receptor (BCR), sequencing was performed for each sample to evaluate antigen receptor repertoires. Samples from healthy volunteers prior to vaccination with BNT162b2 were grouped together with samples from unvaccinated COVID-19-naïve healthy donors as healthy controls (HC).

In total, 123,272 cells from PBMCs from 27 individual samples were obtained, with an average of 4,500 cells/sample. Among these, 36,971 cells (~30%) were from COVID-19 patients, 26,228 cells (~22%) from HCs and pre-vaccine samples, and 60,073 cells (~49%) were from post-immunization samples. All high-quality single cells were integrated across the RNA, antibody-derived tags (ADTs), TCR and BCR modalities for all subsequent analyses. Dimension reduction was performed utilizing the combined RNA and ADT modalities to generate a uniform manifold approximation and projection (UMAP)[30] representation of all 123,272 cells from HC, immunized volunteer and COVID-19 patient samples (Figs. 1A,B). Using a combination of Louvain-based clustering[31], SingleR[32] reference-based annotation, and literature markers we identified 9 major lineages (Fig. 1A and Supplemental Fig. 1A) and 32 individual subpopulations of myeloid cells, B cells, conventional and innate-like T cells, and NK cells (Figs. 1C-F). Gene expression and canonical ADT markers further confirmed these lineages and sub-populations (Supplemental Fig. 1A).

A number of studies have revealed a highly heterogenous picture of the anti-viral inflammatory responses in COVID-19 patients, likely due to variability of disease severity, stage of disease, and diversity of preexisting conditions[2-7]. However, our analysis revealed striking differences in the frequency of several key immune populations between COVID-19 patients and healthy volunteers prior to and following vaccination (Fig. 1). Our multimodal platform enabled us to resolve differences in major immune subsets (Supplemental Fig. 1B), and to resolve rare circulating populations as well (Supplemental Fig. 2). For example, we observed an expansion of circulating hematopoietic stem and progenitor cells (HSPCs) in COVID-19 patients that was absent from healthy volunteers and was not induced by immunization (Supplemental Fig. 1B). Increased frequency of circulating HSPCs is associated with emergency myelopoiesis elicited in response to acute viral infection[33,34]. Consistent with this, and despite the overall heterogeneity in myeloid responses to SARS-CoV-2 in COVID-19 patients, we also observed expansion of several key myeloid populations, including dendritic cell (DC) and monocyte populations (Fig. 1C, Supplemental Fig. 2A).

Myeloid cells are a likely source of type I interferon during SARS-CoV-2 infection

Myeloid cells with high expression of Toll-like receptors (TLR) and other pattern-recognition receptors are likely the first to respond to viral infection. Robust induction of type I IFN through the activation of TLRs constitutes a critical aspect of antiviral immunity. IFN production is dependent on transcription factors IRF7 and IRF8, which interact with MyD88[35-37]. Prior studies of immune responses during COVID-19 found increased activity of these innate immune pathways[38-40]. When we assessed expression of genes associated with IFN production, including IRF7, IRF8, and MyD88 in myeloid cells, plasmacytoid DCs (pDCs) of COVID-19 patients stood out as having high level of expression of these genes (Fig. 2A). Differential gene expression analysis of pDCs from COVID-19 patients and immunized individuals revealed a dramatic upregulation of gene signature associated with type I and type II IFN production in the former and not the latter (Fig 2B). Despite the evident heterogeneity in innate immune responses (Supplemental Fig. 2A), M1 macrophages among COVID-19 patients also stood out as having a marked increase in expression of genes associated with virus-induced IFN production (Supplemental Fig. 3). The observed expansion and transcriptional signatures of these populations are consistent with a role of IFN signaling in initiating inflammatory anti-viral immune responses.

Dramatic difference in maturation of B cell responses triggered by SARS-CoV-2 infection and vaccination

Current COVID-19 vaccine efforts have focused on generation of humoral immune responses against SARS-CoV-2, which was demonstrated to be a correlate of protection against infection[41]. The primary target of neutralizing antibodies is the RBD of the S protein[22,42]. To evaluate antibody responses following COVID-19 infection and immunization, we utilized a Multiplex Bead Binding Assay (MBBA), which permits flow cytometry-based profiling of serum antibodies against multiple viral epitopes[43]. In this assay, we quantified serum IgG, IgA, and IgM antibodies specific to three viral epitopes: S1 domain of spike, RBD, and NC (Fig. 3A,

Supplemental Figs. 4A-C). As expected, anti-NC antibodies were only detected in COVID-19 patients, but not in healthy adults who received the BNT162b2 mRNA vaccine, which encodes only the S protein of SARS-CoV-2 (Supplemental Fig. 4A).

Serums antibody titers were highly variable in COVID-19 patient samples (Fig. 3A, Supplemental Figs. 4A-C), consistent with previous findings[44]. Overall, IgG, IgA, and IgM antibody titers against all viral antigens were higher in late and convalescent samples in all participants for whom longitudinal data were available, except SK-010. In this individual, IgG, IgA, and IgM antibodies against all viral antigens assayed decreased in convalescent samples relative to earlier time points.

Unlike the heterogenous humoral responses in COVID-19 patients, all volunteers who received the vaccine mounted robust IgG, IgA, and IgM antibody responses against S1 and RBD, with serum antibody titers comparable to those seen in COVID-19 patients (Fig. 3A, Supplemental Figs. 4A-C). These responses were evident two weeks after the first vaccine dose and peaked one week after the second dose, consistent with previous reports[45]. IgG antibody levels remained high for at least seven weeks following the first vaccine dose, whereas IgA antibody titers declined steadily beginning one week after the second vaccine dose, although they remained elevated relative to baseline measurements.

To better understand the humoral responses following infection and vaccination, we considered the B cell responses in the CITE-seq dataset (Fig. 1). Single-cell analysis identified five distinct B cell populations based on gene expression and surface epitopes (Fig. 1D). We observe striking expansion of circulating plasmablasts in COVID-19 patients relative to healthy volunteers (Fig. 1D). In contrast, there was no apparent expansion of plasmablasts in circulation following vaccination, despite the clear evidence of a successful humoral response in all subjects (Fig. 3A).

As plasmablasts are likely recent emigrants from lymphoid tissue[46], we hypothesized that they may carry a transcriptional imprint of the inflammatory milieu in tissue. We next performed Gene Set Variation Analysis (GSVA) of plasmablasts from COVID-19 patients and healthy volunteers to ask whether signaling pathways were similarly expressed between these cohorts (Fig. 3B). This analysis revealed that plasmablasts from COVID-19 patients were highly enriched for genes involved in oxidative phosphorylation, type I and type II IFN responses, fatty acid metabolism, and mTORC1 signaling, relative to plasmablasts in healthy volunteers. Plasmablasts from both COVID-19 patients and healthy volunteers following vaccination were enriched for genes involved in IL-6 receptor signaling (JAK/STAT) and inflammatory response, which was consistent with the role of these pathways in promoting plasmablast differentiation[47,48]. Plasmablasts from immunized healthy volunteers were enriched for the transcriptional signature of TNF-NFκB pathway activation. Although signaling pathways among plasmablasts were overall similar in healthy adults and those undergoing vaccination, the increased IFN signaling seen in plasmablasts during acute COVID-19 suggested altered inflammatory milieu in infected patients. These transcriptional changes in response to IFN and other pro-inflammatory cytokines are likely to have broader implications for B cell differentiation and persistence.

The extent of upregulation of IFN response genes in COVID-19 patients correlated with severity of disease, as judged by fraction of inspired oxygen (Fig. 3C) and was consistent with elevated IFN production signature observed in pDCs from these patients. Furthermore, principal component analysis (PCA) of each sample based on the averaged single-cell plasma cell expression of interferon-stimulated[49] transcripts indicated vaccinated and HC samples clustered away from COVID-19 patient samples (Supplemental Fig. 4D). COVID-19 patient samples further separated along PC1 by disease severity and in correlation with expression of *ISG20*, *LY6E*, *BST2* and *STAT1* transcripts which are consistent with IFN-driven responses to viral infection [49,50] (Supplemental Fig. 4, Supplemental Table 1).

We next considered the B cell repertoire across these cohorts. Expansion of B cell clones, as well as convergent antibody repertoires have been reported for a number of viral infections, including SARS-CoV-2[51-55]. Analysis of BCR repertoire revealed that a majority of clonal B lineage cells were captured in the plasmablast cluster in COVID-19 patients. In vaccinated individuals, clonally expanded cells were primarily in naïve and memory compartments (Fig. 3D). This observation suggests that the profound IFN response associated with SARS-CoV-2 infection may promote rapid plasma cell differentiation in COVID-19 patients, while the BNT162b2 mRNA vaccine appears to favor clonal expansion of memory B cells.

To evaluate extent of somatic hypermutation (SHM), we performed IgBlast[56] on the V_H gene repertoire for each individual sample and then evaluated single base-pair mismatches in the full IgH repertoire of various B cell compartments. Increased SHM was apparent in memory B cells from all samples, with frequency of mutations notably higher when compared to naïve B cells from the same samples (Fig. 3E). Frequency of SHMs was significantly reduced in plasmablasts from convalescent COVID-19 samples compared to peak disease (Fig. 3E), possibly as a consequence of long-lived plasma cells migrating out of circulation. Although few plasmablasts were captured in PBMCs from vaccinated individuals, the rate of SHM in plasmablasts and memory B cells in these samples was comparable to that observed from COVID-19 patients at the peak of disease. There was an increase in SHM within the pool of memory cells one week after receiving the second dose of the vaccine compared to one week after receiving the first dose (Fig. 3E). Conspicuously, many of the most mutated variable (V_H) genes in plasmablasts and memory B cells from COVID-19 patients and vaccinated individuals were from V_H gene segments previously implicated in anti-SARS-CoV-2 responses[51,55,57,58] (Fig. 3F). Taken together, these analyses highlight ongoing maturation of B cell responses in both COVID-19 patients and in vaccinated individuals.

Differences in SHM were suggestive of differences in germinal center (GC) biology between cohorts. Induction of effective high-affinity humoral immune responses and generation of memory B cells requires a specialized subset of CD4 Th cells known as T follicular helper (Tfh) cells. Tfh cells are essential for GC formation, affinity maturation, and the generation of most high-affinity antibody-producing and memory B cells[59,60]. A circulating population of Tfh cells, termed circulating Tfh (cTfh), are phenotypically and transcriptionally similar to lymphoid Tfh cells and their presence correlates with ongoing GC reaction and maturation of antibody response[46,61,62]. Indeed, we found significant expansion of the cTfh population in COVID-19 patients relative to healthy volunteers, with a minimal increase in the setting of vaccination (Fig. 1E). GSVA revealed that cells in this population are enriched for genes involved in type I and

type II IFN responses, which were notably absent in cTfh cells found in healthy volunteers (Supplemental Fig. 5). In contrast, cTfh cells from vaccinated individuals were enriched for the transcriptional signature of TNF-NFκB pathway activation, which was associated with improved cTfh survival and more robust humoral immune responses[63].

NK and clonal T cell responses differ in infection and vaccination

Cell-mediated immune responses are carried out by NK cells, CD4 and CD8 T cells, and unconventional T lymphocytes like γδ T cells. In COVID-19 patients, we observed an expansion of cytotoxic populations and a dramatically elevated cytotoxic signature in NK cells, CD4 and CD8 T cells, and γδ T cells (Fig. 4A). A significant increase in the frequency of proliferating T cells and NK cells was also evident in COVID-19 patents, but absent in healthy volunteers and vaccinated individuals (Fig. 4B and Supplemental Figs. 2C,D).

Although CD4 T cells generally help orchestrate and direct effectors of antiviral immune responses, they have also been implicated in direct elimination of infected cells through cytotoxic killing[64-66]. The presence of cytotoxic CD4 T cells has been observed previously in COVID-19 and other viral infections[10,67,68]. We observed an overall depletion of naïve CD4 T cells in COVID-19 patients relative to healthy volunteers, however, activated CD4 T cells were enriched relative to vaccine recipients (Supplemental Fig. 2C). Notably, activated CD4 T cells from COVID-19 patients expressed genes associated with cytotoxic effector function, such as *GZMH*, *GZMA*, and *PRF1* (Fig. 4A).

Successful mobilization of cytotoxic T lymphocytes and NK cells is important for effective antiviral response in COVID-19 and absence of a cytotoxic response may lead to more severe illness[69,70]. Transient lymphopenia is a common feature of many respiratory viral illnesses and has been reported previously in COVID-19[69-72]. Indeed, we observed a significant depletion of total CD8 T cells in COVID-19 patients relative to healthy volunteers (Supplemental Fig. 1B). Our analysis revealed that CD8/CD26 T_{EM} cell population was significantly depleted in COVID-19 patients, while proliferating NK cells were enriched relative to vaccinated individuals (Figs. 1F and 2C,D). Both CD8 effector T cells and NK cells in COVID-19 patients showed significantly elevated expression of genes associated with cytotoxicity, such as *GZMA*, *GZMB*, *GZMH*, *GNLY*, *NKG7*, and *PRF1* (Figs. 4A,B). This was consistent with previous findings that showed a hyperactivation signature in COVID-19, characterized by increased cytotoxicity[73,74]. While clonal expansion was readily evident only among the CD8 effector T cells in COVID-19 patient samples, the BNT162b2 vaccine elicited robust clonal responses in both CD8 effector T cells and in CD8/CD26 T_{EM} cells (Fig.s 4C,E and Supplemental Figs. 6A,B).

γδ T cells are a subset of unconventional non-MHC restricted innate-like T cells with cytotoxic effector functions and ability to regulate other immune cells[75,76]. Interestingly, γδ T cells were enriched in COVID-19 patients, but not in vaccinated individuals (Fig. 1F). Transcriptional analysis revealed expression of genes associated with cytotoxic effector functions in the γδ T cells from COVID-19 patients, a feature that was not observed in γδ T cells from HCs or vaccinated individuals (Fig. 4A). Repertoire analysis of γδ T cells revealed oligoclonal expansion in majority of COVID-19 patients and a moderate dynamic response in vaccinated

individuals (Figs. 4D,F; Supplemental Fig. 6C). Repertoire analysis also highlighted that the majority of larger γδ T cell clones in COVID-19 patients are non-δ2 T cells, and the same held true for vaccinated individuals (Fig. 4F and Supplemental Fig. 6C). In total, we observed expression of genes associated with cytotoxic effector functions among NK cells, CD4 T, CD8 T, and γδ T cells in the setting of COVID-19, which likely contributes to both pathogen clearance and immune-mediated pathology associated with disease.

Discussion

In this study, we performed a highly granular, multimodal analysis of samples from COVID-19 patients and from healthy volunteers before and after receiving the SARS-CoV-2 BNT162b2 mRNA vaccine. While both infection and immunization elicit robust humoral responses, our analysis revealed dramatic differences in cell composition and transcriptional profiles of circulating immune cells in response to the two different immune challenges.

Despite heterogeneity in innate immune response, transcriptional analysis of pDCs and M1 macrophages revealed an upregulation of type I IFN production signature in cells from COVID-19 patients. Type I IFN mediates antiviral immunity, drives expression of a number of genes involved in viral clearance, and plays a critical role in the initiation of innate and adaptive immune responses during a viral infection[77]. Despite extensive antiviral functions, type I IFN signaling can also promote immunopathology through induction of aberrant inflammatory responses during acute viral infection[78,79]. Although the role of type I IFN signaling in COVID-19 remains to be fully elucidated, recent studies show that systemic production of type I IFN is negatively correlated with disease severity and overall outcome[80,81], while excessive local production exacerbates lung tissue damage and correlates with increased morbidity and mortality[82]. Critically, induction of IFNs by viral infection can radically reshape antigen presentation, cellular trafficking, and terminal differentiation of lymphocytes[83,84]. Infection with SARS-CoV-2 potently induced IFN responses, but we did not observe evidence of IFN induction by the BNT162b2 mRNA vaccine.

Both SARS-CoV-2 infection and vaccination were found to elicit SARS-CoV-2-specific antibody responses. While serum IgG levels remained high up to seven weeks after vaccination in all subjects, IgA levels declined. It is thought that the immunological function of IgA is to bind to and neutralize pathogens to prevent infection at mucosal sites, and studies have suggested that IgA contributes to a greater extent to neutralization in SARS-CoV-2 infection than IgG[85]. Murine influenza studies have shown that while IgA prevents infection at mucosal sites in the upper respiratory tract, IgG provides the dominant antibody protection of the lungs after infection has been initiated[86]. Therefore, even if lower IgA response induced by the vaccine is insufficient to prevent infection, it is likely that the robust IgG response restricts viral replication and thus diminishes disease severity and transmission. Prior studies have demonstrated that immunizations at mucosal sites elicit robust IgA responses locally, but fail to generate strong systemic IgA responses, while parenteral challenges induce stronger systemic response but sub-optimal protection at mucosal sites[87]. One recent study suggests that neutralizing antibodies are rarely detected in nasal swabs from subjects who received the BNT162b2 SARS-CoV-2 mRNA vaccine[88], however, it remains to be determined whether the vaccine elicits protective mucosal immunity. Longitudinal assessment of mucosal and systemic humoral immune responses

following immunization would provide valuable information regarding the nature and durability of protective humoral immunity induced by COVID-19 vaccines.

COVID-19 patients had a striking expansion of antibody-producing plasmablasts, with evidence of clonal cells in this cluster. However, we did not detect appreciable expansion of plasmablasts in circulation of individuals immunized with SARS-CoV-2 BNT162b2 mRNA vaccine, despite a robust antibody response. This suggest that antibody-producing cells either migrate to their bone marrow niche at a time not captured by our weekly sampling, or stay resident in the tissues where they were generated. Further studies evaluating the presence of SARS-CoV-2-specific long-lived plasma cells in bone marrow following infection or immunization would shed light on the durability of protective immunity and aid in determining the optimal vaccine schedule and need for booster vaccines against the novel coronavirus in the future.

Recent studies have demonstrated that SARS-CoV-2 mRNA vaccines elicit potent antigen-specific GC responses[18]. We observed extensive accumulation of SHMs in memory B cells and plasma cells from COVID-19 patients, especially in B cells carrying BCR rearrangements that utilized V_H elements previously implicated in anti-SARS-CoV-2 responses[51,55,57,58] (Fig. 3F). Consistent with the idea of long-lived plasma cell trafficking to the bone marrow, convalescent patients have a reduced presence of plasmablasts in circulation, and the SHM footprint in the repertoire of the remaining cells was significantly diminished to what we observed at peak disease. Consistent with our observation of SHMs in plasmablasts and memory B cells from COVID-19 patients, cTfh cells were also readily found among PBMCs from these patients, suggestive of an ongoing GC response. While an earlier study of postmortem thoracic lymph nodes from patients with severe COVID-19 found a block in Tfh differentiation and muted GC response[89], the difference in our observations may be a consequence of studying patients with less severe disease. In contrast, we did not observe an increase in cTfh among individuals that received the mRNA vaccine. It is possible that either our sample collection schedule was not optimal to recover responding cTfh in immunized individuals, or that the systemic, and vastly more complicated, nature of infection generates more robust GC responses than the mRNA vaccine.

In our study, plasmablasts in COVID-19 patients were characterized by a strong type I IFN gene expression signature relative to those in the periphery of healthy volunteers and vaccine recipients. While overzealous IFN response could contribute to abortive GC formation, favoring extrafollicular plasma cell differentiation and sub-optimal maturation of anti-viral responses[90,91], we observed accumulation of SHMs in the repertoire of plasmablasts and memory cells from COVID-19 patients, as well as vaccinated individuals. In COVID-19 patients, clonal responses were most evident among plasmablasts. On the other hand, clonal cells were found within memory and naïve B cell compartments at multiple time points in vaccinated individuals. It is possible that once analysis can be performed on patient samples stratified by disease severity and evaluated alongside a detailed time course following vaccination, we will be able to truly discern the impact of IFN on maturation of GC responses in the context of infection and vaccination.

Another consequence of high IFN activity could be aberrant humoral responses. Whereas SARS-CoV-2 vaccine development has mainly focused on antibody production, the role of antibodies in SARS-CoV-2 infection is less clear. Strong antibody responses often correlate with more severe

illness and antibody-dependent enhancement of pathology has been described in COVID-19 patients[17,92-96]. In our study, antibody-producing cells were characterized by a type I IFN gene expression signature. A strong IFN signature has been associated with pathogenic autoantibodies in systemic lupus erythematosus (SLE)[97,98]. Previous studies have highlighted the shared IFN-induced gene signature in lymphocytes from patients with autoimmune disease and in subjects following viral infections[98,99]. Our observation that B lymphocyte transcriptional programs in COVID-19 patients are dominated by dramatic upregulation of IFN-response genes may be important for understanding the immunopathology of COVID-19, as there is growing evidence that autoantibodies could be driving severe disease and long-term sequelae in some COVID-19 patients[92-94,96].

Recent studies emphasize generation of antigen-specific T cells in protective immunity against SARS-CoV-2 infection and it is becoming increasingly clear that successful vaccines need to engage the cellular adaptive immune response[100-102]. Indeed, humoral immune responses may be less effective against new SARS-CoV-2 variants[88,103]. Conversely, SARS-CoV-2-specific CD8 T cell responses, which target a broad range of epitopes, remain largely intact against new variants presently in circulation[104]. Our analysis revealed that both SARS-CoV-2 infection and, to a lesser degree, vaccination elicit clonal CD8 effector T cell responses. We also observed a strong clonal response in CD8/CD26 T_{EM} cells in all volunteers following immunization – a feature of adaptive response that was notably absent in COVID-19 patients. Robust SARS-CoV-2-specific T cell immunity is maintained for up to eight months after infection, but as yet it is not clear how durable T cell responses are following vaccination[15]. However, the clonal expansion of CD8 T_{EM} cells we observed in vaccinated volunteers suggests that vaccination elicits memory T cell responses, which are likely to be long-lived.

Peripheral immune cells of COVID-19 patients were enriched in T cells, NK cells, and γδ T cells with a highly activated phenotype and elevated expression of genes associated with cytotoxic effector functions (*GZMA*, *GZMB*, *GZMH*, *PRF1*, *GNLY*, *NKG7*, and *IL-32*). We observed the presence of cytotoxic CD4 T cells in COVID-19 patients that were largely absent in healthy volunteers following immunization. While hyperactivation of inflammatory responses and cytotoxic cells may contribute to immunopathology in severe illness, in mild and moderate disease, these features are indicative of protective immune responses and resolution of infection[71,105]. A multi-cohort analysis of immune responses across different viral infections showed that increased frequency of NK cells and expression of NK-associated genes is inversely correlated with severity[106]. This is consistent with previous studies that show that reduced NK frequency and function are associated with increased tissue damage and severe COVID-19[107].

Our study, together with others, underscores the fine balance between antiviral immune responses that achieve clearance of the infection and durable protective immunity, and those that lead to inflammation and immunopathology. Better understanding of the immunological features associated with protective immunity, immunopathology, and durability of protective immunological memory will aid not only in better treatments for viral diseases, but also facilitate the rapid development of effective vaccines for new and re-emerging viral diseases that threaten public health.

Materials and methods

Patients and sample collection

Peripheral blood samples were drawn from both outpatients and hospitalized patients with confirmed COVID-19 at NYU Langone Health. SARS-CoV-2 was detected in patients' nasopharyngeal swab using the Cobras SARS-CoV-2 real time PCR under EUA. Peripheral blood was collected in accordance with a NYU Institutional Review Board protocols (IRB 18-02035, 18-02037 and 20-00463). Samples were de-identified and assigned coded identification numbers prior to analysis.

Whole blood was collected in commercially-available heparin-coated tubes (BD). Plasma was collected from whole blood by centrifugation at 2000 x *g* at 4°C, aliquoted, and stored at -20°C. For serum collection, whole blood was collected in a serum separator tube (SST) tubes (BD). The blood was allowed to clot undisturbed at room temperature for 30-45 minutes and the clot was removed by centrifugation at 2000 x *g* at 4°C, the serum aliquoted and stored at -20°C.

PBMC isolation

PBMCs were isolated from peripheral blood by diluting whole blood in gradient centrifugation using Ficoll-Paque PLUS (GE Healthcare) and SepMate™ PBMC Isolation Tubes (Stemcell) according to the manufacturer's instructions. Buffy coat PBMCs were cryopreserved in FBS supplemented with 10% DMSO and stored in liquid nitrogen.

Single-cell RNA-seq

Single cell transcriptome profiling of PBMCs was carried out using the Chromium Next GEM Single Cell 5' Library & Gel Bead Kit (v1.1) and Chromium controller (10X Genomics). PBMCs were thawed and live cells were enriched using Miltenyi Live Enrichment Kit to ensure viability of all samples is over 95% prior to staining. To enable multiplexing and doublet detection, cells were stained with barcoded antibodies for CITE-seq and cell hashing described previously [26,27,29,108]. Expression of selected surface protein markers (previously titrated antibody panel in supplemental materials) [29] was achieved by staining with barcoded antibodies as described[27]. Briefly, approximately 200,000 cells per sample were resuspended in staining buffer (PBS, 2% BSA, 0.01% Tween) and incubated for 10 minutes with Fc block (TruStain FcX, Biolegend; FcR blocking reagent, Miltenyi). Cells were then incubated with barcoded antibodies for 30 min at 4 °C. After staining, cells were washed 3 times in staining buffer. After the final wash, cells were resuspended in PBS + 0.04% BSA, filtered, and counted. Cells were pooled and loaded onto the Chromium chips (5 samples per lane, targeting 5,000 cells per sample). The single-cell capturing, barcoding, and cDNA library preparation were performed using the Chromium Next GEM Single Cell 5' Library & Gel Bead Kit following the protocols recommended by the manufacturer. HTO and ADT additive oligonucleotides were spiked into the cDNA amplification PCR and the ADT and HTO libraries were prepared as described previously [27,108]. The cDNA fraction was processed according to the 10x Genomics Single Cell V(D)J protocol to generate the transcriptome library and the TCRα/β and BCR libraries. To amplify TCRγ/δ transcripts, we utilized a two-step PCR similar to TCRα/β approach described

previously [26]. Libraries were pooled to desired quantities and sequenced on a NovaSeq 6000 (S2 flowcell: recipe 26 cycles read 1, 8 cycles index, 91 cycles read 2). Reads were trimmed as required for downstream processing.

Single cell RNA-seq data processing

The Cellranger software suite (https://support.10xgenomics.com/single-cell-gene-expression/software/pipelines/latest/what-is-cell-ranger) from 10X was used to demultiplex cellular barcodes, align reads to the human genome (GRCh38 ensemble, http://useast.ensembl.org/Homo_sapiens/Info/Index) and perform UMI counting. ADT and HTO count matrices were generated by kallisto kb-count v0.24.1[109,110] and HTOs demultiplexed by HTODemux from Seurat v4.0.0[111]. Following cellranger all other processing was performed in R v4.0.3[112]. From filtered counts Seurat was used to process the single cell data, generate UMAP representation based on totalVI[113] dimension reduction of RNA and ADT modalities. RNA was normalized and batch-corrected by totalVI, while ADT values were corrected by the built-in integration function FindIntegrationAnchors in Seurat. Clustering was performed by the Louvain algorithm[31] and cell type identification was determined by clustering, SingleR annotations, corrected ADT levels and canonical markers for various immune cell subsets. Further sub-clustering was performed on Myeloid, B, conventional T and innate-like T and NK cells to identify 32 individual populations. BCR/TCR sequences were processed by cellranger VDJ and added to the metadata of the combined Seurat object for each sample. Statistical differences in cell type clusters in all instances was determined by a Wilcoxon test. GSVA of select immune cell subsets were performed in R with the GSVA package v1.38[114] with various named gene sets from MSigDB (http://www.gsea-msigdb.org/gsea/index.jsp). Differential expression between cell types and between cells from HC, immunized individuals and COVID-19 samples were also assessed by Wilcox test with Benjamin-Hochberg p-value adjustment.

Multiplex bead-binding assay for antibody profiling

Multiplex bead-binding assay was carried out as described [43], with the following modifications. Briefly, we produced the spike and RBD proteins as described [43] and purchased biotinylated nucleocapsid protein (Sino Biological, catalog number 40588-V27B-B). We used MultiCyt® QBeads® Streptavidin Coated panel QSAv1,2,3 and 5 (Sartorius catalog number 90792) to immobilize SARS-CoV-2 antigens; Spike to QSAv1, Nucleocapsid to QSAv2, the receptor-binding-domain of Spike (RBD) to QSAv3, and biotin only to QSAv5. The antigens were diluted to 25 nM in PBS with 0.5 % BSA and mixed with the same volume of the twice-washed QBeads. We detected antigen-specific antibodies in heat-inactivated serum or plasma using anti-human IgG-Alexa 488 (Jackson Immunoresearch; catalog number 109-545-098, 1:800 in PBS 0.1 % Tween 20 and with 1 % BSA), anti-human IgA-PE (Jackson Immunoresearch; catalog number 109-115-011, 1:100) and anti-human IgM-DyLight405 (Jackson Immunoresearch; catalog number 709-475-073, 1:200). We measured the samples on a Yeti ZE5 Cell Analyzer (Bio-Rad) and analyzed the data using FlowJo (BD, version 10.7.1).

Acknowledgements

We are grateful for support of this work from NYU Grossman School of Medicine. Work in Dr. Koralov's laboratory was further supported by the NIH R01 grant (HL-125816), LEO Foundation Grant (LF-OC-20-000351), NYU Cancer Center Pilot Grant (P30CA016087), the Judith and Stewart Colton Center for Autoimmunity Pilot grant. Presented work was also supported by NIH grant R21 AI158997, R01 CA194864 and R01 CA212608 to S.K.; NIH grants AI114852 and AI082630 to R.S.H.; and AI148574 to M.J.M. TBB and NØ are supported by the Danish Cancer Society (Kræftens Bekæmpelse), the Danish Council for Independent Research (Danmarks Frie Forskningsfond) and the LEO Foundation. We thank the NYU Vaccine Center team, everyone at NYU Genome Technology Center, and Dr. Heguy in particular, for technical assistance and support.

Disclosures

MJM reported potential competing interests: laboratory research and clinical trials contracts with Lilly, Pfizer (exclusive of the current work), and Sanofi for vaccines or MAB vs SARS-CoV-2; contract funding from USG/HHS/BARDA for research specimen characterization and repository; research grant funding from USG/HHS/NIH for SARS-CoV-2 vaccine and MAB clinical trials; personal fees from Meissa Vaccines, Inc. and Pfizer for Scientific Advisory Board service.

Figure Legends

Figure 1. Single-cell landscape of immunological responses to COVID-19 and SARS-CoV-2 BNT162b2 mRNA vaccine

a. UMAP representation of over 123,000 PBMCs by scRNA-seq, clustered and colored by indicated cell type. Clusters identified based on gene expression and surface epitopes.

b. UMAP visualization of PBMCs from and COVID-19-naïve healthy donors (blue), healthy volunteers before receiving the BNT162b2 mRNA vaccine (blue), healthy volunteers after receiving the BNT162b2 mRNA vaccine (orange), and COVID-19 patients (red).

c-f. UMAP representation of subclustered myeloid (**c**), B cell (**d**), T cell (**e**), and innate and unconventional T cell (**f**) populations colored and labeled by cell type. Boxplots highlight specific populations that exhibited significant differences between healthy volunteers and COVID-19 patients. P-values are determined by a Wilcox test.

Figure 2. Myeloid cell expression of type I interferon pathway.

a. Scaled normalized expression of *IRF7*, *IRF8*, and *LILRA4* in 8 identified myeloid populations (left) and plotted for specific expression in pDCs from HC, Vaccine samples and COVID-19 patients (right).

b. Scaled and normalized expression of IFN production-associated genes in pDCs based on gene ontology (GO) gene set for type I IFN production (GO:0032606).

Figure 3. Maturation of B cell responses

a. SARS-CoV-2-specific antibody titers were assessed for COVID-19 patients and healthy volunteers using a Multiplex Bead Binding Assay (MBBA). We assayed IgG, IgA, and IgM antibody titers specific for SARS-CoV-2 Spike, RBD, and NC. Anti-RBD IgG (top) and IgA (bottom) are shown for COVID-19 patients and healthy donors (left), and for healthy volunteers who received the SARS-CoV-2 BNT162b2 mRNA vaccine (right), colored by subject. COVID-19 patient samples were split into early/acute (<8 DPO), late (8-13 DPO), and convalescent (>13DPO). Connected lines indicate repeated measurements for the same subjects.

b. GSVA analysis of plasmablasts in cells from HC, Vaccine and COVID-19 (bottom color bar) patients from the Hallmark gene set[115] and colored by oxygen requirement (top color bar) which is a clinical parameter defined as the fraction of inspired oxygen, where 21% represents oxygen content of room air without supplementation. Vaccine and HC cells are colored at 21%.

c. Oxygen requirement against GSVA enrichment score for interferon alpha response gene set as shown in b. p and tau values are determined by a Kendall rank correlation test.

d. Clonal populations based on individual B cell IGH chain CDR3 sequence. CDR3 sequences occurring in at least 2 cells are colored blue, while any CDR3 sequences in at least 3 cells are colored uniquely in cells from Vaccinated (top) and COVID-19 patient samples (bottom)

e. Number of mismatched bases according to IgBlast results of recovered V_H gene sequences in plasmablasts (top) memory (middle) and naïve (bottom) B cell subsets in cells from HC, Vaccinated and COVID-19 patient samples. P-value were determined by Wilcox test.

f. Frequency of highly mutated V_H gene sequences in experienced memory and plasmablasts. Frequency is normalized by the total number of memory and plasmablasts in each patient group. Asterisks indicate V_H gene sequences previously implicated in SARS-CoV-2 infection and vaccination[51,55,57,58].

Figure 4. Cytotoxic responses and clonality of conventional and innate-like T cells in COVID-19 and SARS-CoV-2 vaccine recipients

a. Boxplots of cell percentages of select cytotoxic cell populations that exhibited significant differences between COVID-19-naïve donors and healthy volunteers before receiving the BNT162b2 mRNA vaccine (blue), healthy volunteers after receiving the BNT162b2 mRNA vaccine (orange), and COVID-19 patients (red). P-values are determined by a Wilcox test.

b. Average per-sample scaled expression of genes associated with cytotoxic effector function from the gene set T cell mediated cytotoxicity (GO:0001913).

c. UMAP visualization of clonal CD8 T cells from COVID-19 patients (left) and healthy volunteers after receiving the BNT162b2 mRNA vaccine (right). Clonality is determined by the CDR3 sequence in TCRβ chain. Identical CDR3 sequences in at least 3 cells are colored uniquely.

d. UMAP visualization of clonal γδT cells from COVID-19 patients (left) and healthy volunteers after receiving the BNT162b2 mRNA vaccine (right). Clonality is determined by the CDR3 sequence in TCRδ chain. Identical CDR3 sequences in at least 3 cells are colored uniquely.

e. Bar graphs showing clonal repertoire distribution among CD8 T_{EM} and T_{eff} cells based on TCRβ CDR3 sequence in one representative sample set from acute COVID-19 patient and from time course of a vaccinated individual. Polyclonal cells in grey. Circos plots of frequencies of Vβ and Jβ usage are shown and colored uniquely by CDR3 sequences as in c.

f. Bar graphs showing clonal repertoire distribution among γδ T cells based on TCRδ CDR3 sequence in one representative sample set from acute COVID-19 patient and from time course of a vaccinated individual. Polyclonal cells in grey. Circos plots of frequencies of Vδ and Jδ usage is shown and colored uniquely by CDR3 sequences as in d.

References:

1 Dong, E., Du, H. & Gardner, L. An interactive web-based dashboard to track COVID-19 in real time. *Lancet Infect Dis* **20**, 533-534, doi:10.1016/s1473-3099(20)30120-1 (2020).

2 Desai, N. *et al.* Temporal and spatial heterogeneity of host response to SARS-CoV-2 pulmonary infection. *Nature Communications* **11**, 6319, doi:10.1038/s41467-020-20139-7 (2020).

3 Mathew, D. *et al.* Deep immune profiling of COVID-19 patients reveals distinct immunotypes with therapeutic implications. *Science* **369**, eabc8511, doi:10.1126/science.abc8511 (2020).

4 Merad, M. & Martin, J. C. Pathological inflammation in patients with COVID-19: a key role for monocytes and macrophages. *Nature Reviews Immunology* **20**, 355-362, doi:10.1038/s41577-020-0331-4 (2020).

5 Singh, R. *et al.* Sustained expression of inflammatory monocytes and activated T cells in COVID-19 patients and recovered convalescent plasma donors. *medRxiv*, 2020.2011.2017.20233668, doi:10.1101/2020.11.17.20233668 (2020).

6 Wilk, A. J. *et al.* A single-cell atlas of the peripheral immune response in patients with severe COVID-19. *Nature Medicine* **26**, 1070-1076, doi:10.1038/s41591-020-0944-y (2020).

7 Zheng, J. *et al.* Severe Acute Respiratory Syndrome Coronavirus 2-Induced Immune Activation and Death of Monocyte-Derived Human Macrophages and Dendritic Cells. *J Infect Dis* **223**, 785-795, doi:10.1093/infdis/jiaa753 (2021).

8 Kared, H. *et al.* SARS-CoV-2–specific CD8+ T cell responses in convalescent COVID-19 individuals. *The Journal of Clinical Investigation* **131**, doi:10.1172/JCI145476 (2021).

9 Le Bert, N. *et al.* SARS-CoV-2-specific T cell immunity in cases of COVID-19 and SARS, and uninfected controls. *Nature* **584**, 457-462, doi:10.1038/s41586-020-2550-z (2020).

10 Zhang, J.-Y. *et al.* Single-cell landscape of immunological responses in patients with COVID-19. *Nature Immunology* **21**, 1107-1118, doi:10.1038/s41590-020-0762-x (2020).

11 Zuo, J. *et al.* Robust SARS-CoV-2-specific T cell immunity is maintained at 6 months following primary infection. *Nature Immunology*, doi:10.1038/s41590-021-00902-8 (2021).

12 Jeewandara, C. *et al.* SARS-CoV-2 neutralizing antibodies in patients with varying severity of acute COVID-19 illness. *Scientific Reports* **11**, 2062, doi:10.1038/s41598-021-81629-2 (2021).

13 Wang, X. *et al.* Neutralizing Antibody Responses to Severe Acute Respiratory Syndrome Coronavirus 2 in Coronavirus Disease 2019 Inpatients and Convalescent Patients. *Clin Infect Dis* **71**, 2688-2694, doi:10.1093/cid/ciaa721 (2020).

14 Chodick, G. *et al.* The effectiveness of the first dose of BNT162b2 vaccine in reducing SARS-CoV-2 infection 13-24 days after immunization: real-world evidence. *medRxiv*, 2021.2001.2027.21250612, doi:10.1101/2021.01.27.21250612 (2021).

15 Dan, J. M. *et al.* Immunological memory to SARS-CoV-2 assessed for up to 8 months after infection. *Science* **371**, eabf4063, doi:10.1126/science.abf4063 (2021).

16 Thompson, M. G. *et al.* Interim Estimates of Vaccine Effectiveness of BNT162b2 and mRNA-1273 COVID-19 Vaccines in Preventing SARS-CoV-2 Infection Among Health Care Personnel, First Responders, and Other Essential and Frontline Workers - Eight U.S.

Locations, December 2020-March 2021. *MMWR Morb Mortal Wkly Rep* **70**, 495-500, doi:10.15585/mmwr.mm7013e3 (2021).

17 Cervia, C. *et al.* Systemic and mucosal antibody responses specific to SARS-CoV-2 during mild versus severe COVID-19. *J Allergy Clin Immunol* **147**, 545-557.e549, doi:10.1016/j.jaci.2020.10.040 (2021).

18 Lederer, K. *et al.* SARS-CoV-2 mRNA Vaccines Foster Potent Antigen-Specific Germinal Center Responses Associated with Neutralizing Antibody Generation. *Immunity* **53**, 1281-1295.e1285, doi:10.1016/j.immuni.2020.11.009 (2020).

19 Wu, J. *et al.* SARS-CoV-2 infection induces sustained humoral immune responses in convalescent patients following symptomatic COVID-19. *Nature Communications* **12**, 1813, doi:10.1038/s41467-021-22034-1 (2021).

20 Sherina, N. *et al.* Persistence of SARS-CoV-2-specific B and T cell responses in convalescent COVID-19 patients 6–8 months after the infection. *Med* **2**, 281-295.e284, doi:https://doi.org/10.1016/j.medj.2021.02.001 (2021).

21 Satarker, S. & Nampoothiri, M. Structural Proteins in Severe Acute Respiratory Syndrome Coronavirus-2. *Arch Med Res* **51**, 482-491, doi:10.1016/j.arcmed.2020.05.012 (2020).

22 Tai, W. *et al.* Characterization of the receptor-binding domain (RBD) of 2019 novel coronavirus: implication for development of RBD protein as a viral attachment inhibitor and vaccine. *Cellular & Molecular Immunology* **17**, 613-620, doi:10.1038/s41423-020-0400-4 (2020).

23 Hsieh, C. L. *et al.* Structure-based design of prefusion-stabilized SARS-CoV-2 spikes. *Science* **369**, 1501-1505, doi:10.1126/science.abd0826 (2020).

24 Vogel, A. B. *et al.* A prefusion SARS-CoV-2 spike RNA vaccine is highly immunogenic and prevents lung infection in non-human primates. *bioRxiv*, 2020.2009.2008.280818, doi:10.1101/2020.09.08.280818 (2020).

25 Bos, R. *et al.* Ad26 vector-based COVID-19 vaccine encoding a prefusion-stabilized SARS-CoV-2 Spike immunogen induces potent humoral and cellular immune responses. *NPJ Vaccines* **5**, 91, doi:10.1038/s41541-020-00243-x (2020).

26 Mimitou, E. P. *et al.* Multiplexed detection of proteins, transcriptomes, clonotypes and CRISPR perturbations in single cells. *Nature Methods* **16**, 409-412, doi:10.1038/s41592-019-0392-0 (2019).

27 Stoeckius, M. *et al.* Simultaneous epitope and transcriptome measurement in single cells. *Nature methods* **14**, 865-868, doi:10.1038/nmeth.4380 (2017).

28 WHO Working Group on the Clinical Characterisation and Management of COVID-19 infection. A minimal common outcome measure set for COVID-19 clinical research. *Lancet Infect Dis* **20**, e192-e197, doi:10.1016/s1473-3099(20)30483-7 (2020).

29 Buus, T. B. *et al.* Improving oligo-conjugated antibody signal in multimodal single-cell analysis. *bioRxiv*, 2020.2006.2015.153080, doi:10.1101/2020.06.15.153080 (2020).

30 McInnes, L. & Healy, J. UMAP: Uniform Manifold Approximation and Projection for Dimension Reduction. *ArXiv* **abs/1802.03426** (2018).

31 Blondel, V. D., Guillaume, J.-L., Lambiotte, R. & Lefebvre, E. Fast unfolding of communities in large networks. *Journal of Statistical Mechanics: Theory and Experiment* **2008**, P10008, doi:10.1088/1742-5468/2008/10/p10008 (2008).

32 Aran, D. *et al.* Reference-based analysis of lung single-cell sequencing reveals a transitional profibrotic macrophage. *Nature Immunology* **20**, 163-172, doi:10.1038/s41590-018-0276-y (2019).

33 Schürch, C. M., Riether, C. & Ochsenbein, A. F. Cytotoxic CD8+ T cells stimulate hematopoietic progenitors by promoting cytokine release from bone marrow mesenchymal stromal cells. *Cell Stem Cell* **14**, 460-472, doi:10.1016/j.stem.2014.01.002 (2014).

34 Takizawa, H., Boettcher, S. & Manz, M. G. Demand-adapted regulation of early hematopoiesis in infection and inflammation. *Blood* **119**, 2991-3002, doi:10.1182/blood-2011-12-380113 (2012).

35 Lester, S. N. & Li, K. Toll-like receptors in antiviral innate immunity. *J Mol Biol* **426**, 1246-1264, doi:10.1016/j.jmb.2013.11.024 (2014).

36 Tailor, P. *et al.* The feedback phase of type I interferon induction in dendritic cells requires interferon regulatory factor 8. *Immunity* **27**, 228-239, doi:10.1016/j.immuni.2007.06.009 (2007).

37 Xagorari, A. & Chlichlia, K. Toll-like receptors and viruses: induction of innate antiviral immune responses. *Open Microbiol J* **2**, 49-59, doi:10.2174/1874285800802010049 (2008).

38 Scagnolari, C. *et al.* Differential induction of type I and III interferon genes in the upper respiratory tract of patients with coronavirus disease 2019 (COVID-19). *Virus Research* **295**, 198283, doi:https://doi.org/10.1016/j.virusres.2020.198283 (2021).

39 Xu, G. *et al.* The differential immune responses to COVID-19 in peripheral and lung revealed by single-cell RNA sequencing. *Cell Discovery* **6**, 73, doi:10.1038/s41421-020-00225-2 (2020).

40 Zhou, Z. *et al.* Heightened Innate Immune Responses in the Respiratory Tract of COVID-19 Patients. *Cell Host Microbe* **27**, 883-890.e882, doi:10.1016/j.chom.2020.04.017 (2020).

41 McMahan, K. *et al.* Correlates of protection against SARS-CoV-2 in rhesus macaques. *Nature* **590**, 630-634, doi:10.1038/s41586-020-03041-6 (2021).

42 Premkumar, L. *et al.* The receptor-binding domain of the viral spike protein is an immunodominant and highly specific target of antibodies in SARS-CoV-2 patients. *Science Immunology* **5**, eabc8413, doi:10.1126/sciimmunol.abc8413 (2020).

43 Hattori, T. *et al.* Multiplex bead binding assays using off-the-shelf components and common flow cytometers. *Journal of Immunological Methods* **490**, 112952, doi:https://doi.org/10.1016/j.jim.2020.112952 (2021).

44 Noval, M. G. *et al.* Antibody isotype diversity against SARS-CoV-2 is associated with differential serum neutralization capacities. *Sci Rep* **11**, 5538, doi:10.1038/s41598-021-84913-3 (2021).

45 Ebinger, J. E. *et al.* Antibody responses to the BNT162b2 mRNA vaccine in individuals previously infected with SARS-CoV-2. *Nature Medicine*, doi:10.1038/s41591-021-01325-6 (2021).

46 Vella, L. A. *et al.* T follicular helper cells in human efferent lymph retain lymphoid characteristics. *J Clin Invest* **129**, 3185-3200, doi:10.1172/jci125628 (2019).

47 Hirano, T., Ishihara, K. & Hibi, M. Roles of STAT3 in mediating the cell growth, differentiation and survival signals relayed through the IL-6 family of cytokine receptors. *Oncogene* **19**, 2548-2556, doi:10.1038/sj.onc.1203551 (2000).

48 Rodríguez-Bayona, B., Ramos-Amaya, A., López-Blanco, R., Campos-Caro, A. & Brieva, J. A. STAT-3 activation by differential cytokines is critical for human in vivo-generated plasma cell survival and Ig secretion. *J Immunol* **191**, 4996-5004, doi:10.4049/jimmunol.1301559 (2013).

49 Liu, S.-Y., Sanchez, D. J., Aliyari, R., Lu, S. & Cheng, G. Systematic identification of type I and type II interferon-induced antiviral factors. *Proceedings of the National Academy of Sciences* **109**, 4239-4244, doi:10.1073/pnas.1114981109 (2012).

50 Kane, M. *et al.* Identification of Interferon-Stimulated Genes with Antiretroviral Activity. *Cell Host Microbe* **20**, 392-405, doi:10.1016/j.chom.2016.08.005 (2016).

51 Gaebler, C. *et al.* Evolution of antibody immunity to SARS-CoV-2. *Nature* **591**, 639-644, doi:10.1038/s41586-021-03207-w (2021).

52 Jackson, K. J. *et al.* Human responses to influenza vaccination show seroconversion signatures and convergent antibody rearrangements. *Cell Host Microbe* **16**, 105-114, doi:10.1016/j.chom.2014.05.013 (2014).

53 Nielsen, S. C. A. *et al.* Human B Cell Clonal Expansion and Convergent Antibody Responses to SARS-CoV-2. *Cell Host & Microbe* **28**, 516-525.e515, doi:https://doi.org/10.1016/j.chom.2020.09.002 (2020).

54 Parameswaran, P. *et al.* Convergent antibody signatures in human dengue. *Cell Host Microbe* **13**, 691-700, doi:10.1016/j.chom.2013.05.008 (2013).

55 Robbiani, D. F. *et al.* Convergent antibody responses to SARS-CoV-2 in convalescent individuals. *Nature* **584**, 437-442, doi:10.1038/s41586-020-2456-9 (2020).

56 Ye, J., Ma, N., Madden, T. L. & Ostell, J. M. IgBLAST: an immunoglobulin variable domain sequence analysis tool. *Nucleic Acids Research* **41**, W34-W40, doi:10.1093/nar/gkt382 (2013).

57 Brouwer, P. J. M. *et al.* Potent neutralizing antibodies from COVID-19 patients define multiple targets of vulnerability. *Science* **369**, 643-650, doi:10.1126/science.abc5902 (2020).

58 Wang, Z. *et al.* mRNA vaccine-elicited antibodies to SARS-CoV-2 and circulating variants. *Nature*, doi:10.1038/s41586-021-03324-6 (2021).

59 Crotty, S. T Follicular Helper Cell Biology: A Decade of Discovery and Diseases. *Immunity* **50**, 1132-1148, doi:10.1016/j.immuni.2019.04.011 (2019).

60 Stebegg, M. *et al.* Regulation of the Germinal Center Response. *Frontiers in Immunology* **9**, doi:10.3389/fimmu.2018.02469 (2018).

61 Bentebibel, S. E. *et al.* Induction of ICOS+CXCR3+CXCR5+ TH cells correlates with antibody responses to influenza vaccination. *Sci Transl Med* **5**, 176ra132, doi:10.1126/scitranslmed.3005191 (2013).

62 Herati, R. S. *et al.* Successive annual influenza vaccination induces a recurrent oligoclonotypic memory response in circulating T follicular helper cells. *Science Immunology* **2**, eaag2152, doi:10.1126/sciimmunol.aag2152 (2017).

63 Herati, R. S. *et al.* Vaccine-induced ICOS+CD38+ cTfh are sensitive biosensors of age-related changes in inflammatory pathways. *bioRxiv*, 711911, doi:10.1101/711911 (2019).

64 Sun, B. & Zhang, Y. Overview of orchestration of CD4+ T cell subsets in immune responses. *Adv Exp Med Biol* **841**, 1-13, doi:10.1007/978-94-017-9487-9_1 (2014).

65 Swain, S. L., McKinstry, K. K. & Strutt, T. M. Expanding roles for CD4+ T cells in immunity to viruses. *Nature Reviews Immunology* **12**, 136-148, doi:10.1038/nri3152 (2012).

66 Takeuchi, A. & Saito, T. CD4 CTL, a Cytotoxic Subset of CD4(+) T Cells, Their Differentiation and Function. *Frontiers in immunology* **8**, 194-194, doi:10.3389/fimmu.2017.00194 (2017).

67 Meckiff, B. J. *et al.* Imbalance of Regulatory and Cytotoxic SARS-CoV-2-Reactive CD4(+) T Cells in COVID-19. *Cell* **183**, 1340-1353.e1316, doi:10.1016/j.cell.2020.10.001 (2020).

68 Juno, J. A. *et al.* Cytotoxic CD4 T Cells-Friend or Foe during Viral Infection? *Front Immunol* **8**, 19, doi:10.3389/fimmu.2017.00019 (2017).

69 Odak, I. *et al.* Reappearance of effector T cells is associated with recovery from COVID-19. *EBioMedicine* **57**, 102885, doi:https://doi.org/10.1016/j.ebiom.2020.102885 (2020).

70 Westmeier, J. *et al.* Impaired Cytotoxic CD8⁺ T Cell Response in Elderly COVID-19 Patients. *mBio* **11**, e02243-02220, doi:10.1128/mBio.02243-20 (2020).

71 Chen, Z. & John Wherry, E. T cell responses in patients with COVID-19. *Nature Reviews Immunology* **20**, 529-536, doi:10.1038/s41577-020-0402-6 (2020).

72 Cheng, Y. *et al.* Dynamic changes of lymphocyte counts in adult patients with severe pandemic H1N1 influenza A. *Journal of Infection and Public Health* **12**, 878-883, doi:https://doi.org/10.1016/j.jiph.2019.05.017 (2019).

73 Kuri-Cervantes, L. *et al.* Comprehensive mapping of immune perturbations associated with severe COVID-19. *Science Immunology* **5**, eabd7114, doi:10.1126/sciimmunol.abd7114 (2020).

74 Yu, K. *et al.* Dysregulated adaptive immune response contributes to severe COVID-19. *Cell Research* **30**, 814-816, doi:10.1038/s41422-020-0391-9 (2020).

75 Sabbaghi, A. *et al.* Role of γδ T cells in controlling viral infections with a focus on influenza virus: implications for designing novel therapeutic approaches. *Virology Journal* **17**, 174, doi:10.1186/s12985-020-01449-0 (2020).

76 Lawand, M., Déchanet-Merville, J. & Dieu-Nosjean, M.-C. Key Features of Gamma-Delta T-Cell Subsets in Human Diseases and Their Immunotherapeutic Implications. *Frontiers in Immunology* **8**, doi:10.3389/fimmu.2017.00761 (2017).

77 Wu, W. & Metcalf, J. P. The Role of Type I IFNs in Influenza: Antiviral Superheroes or Immunopathogenic Villains? *Journal of Innate Immunity* **12**, 437-447, doi:10.1159/000508379 (2020).

78 Major, J. *et al.* Type I and III interferons disrupt lung epithelial repair during recovery from viral infection. *Science* **369**, 712, doi:10.1126/science.abc2061 (2020).

79 Teijaro, J. R. Type I interferons in viral control and immune regulation. *Curr Opin Virol* **16**, 31-40, doi:10.1016/j.coviro.2016.01.001 (2016).

80 Hadjadj, J. *et al.* Impaired type I interferon activity and inflammatory responses in severe COVID-19 patients. *Science* **369**, 718, doi:10.1126/science.abc6027 (2020).

81 Liu, C. *et al.* Time-resolved systems immunology reveals a late juncture linked to fatal COVID-19. *Cell* **184**, 1836-1857.e1822, doi:10.1016/j.cell.2021.02.018 (2021).

82 Broggi, A. *et al.* Type III interferons disrupt the lung epithelial barrier upon viral recognition. *Science* **369**, 706, doi:10.1126/science.abc3545 (2020).

83 Gessani, S., Conti, L., Del Cornò, M. & Belardelli, F. Type I interferons as regulators of human antigen presenting cell functions. *Toxins (Basel)* **6**, 1696-1723, doi:10.3390/toxins6061696 (2014).

84 Malmgaard, L. Induction and regulation of IFNs during viral infections. *J Interferon Cytokine Res* **24**, 439-454, doi:10.1089/1079990041689665 (2004).
85 Sterlin, D. *et al.* IgA dominates the early neutralizing antibody response to SARS-CoV-2. *Science Translational Medicine* **13**, eabd2223, doi:10.1126/scitranslmed.abd2223 (2021).
86 Renegar, K. B., Small, P. A., Jr., Boykins, L. G. & Wright, P. F. Role of IgA versus IgG in the control of influenza viral infection in the murine respiratory tract. *J Immunol* **173**, 1978-1986, doi:10.4049/jimmunol.173.3.1978 (2004).
87 Macpherson, A. J., McCoy, K. D., Johansen, F. E. & Brandtzaeg, P. The immune geography of IgA induction and function. *Mucosal Immunology* **1**, 11-22, doi:10.1038/mi.2007.6 (2008).
88 Planas, D. *et al.* Sensitivity of infectious SARS-CoV-2 B.1.1.7 and B.1.351 variants to neutralizing antibodies. *Nature Medicine*, doi:10.1038/s41591-021-01318-5 (2021).
89 Kaneko, N. *et al.* Loss of Bcl-6-Expressing T Follicular Helper Cells and Germinal Centers in COVID-19. *Cell* **183**, 143-157.e113, doi:10.1016/j.cell.2020.08.025 (2020).
90 Braun, D., Caramalho, I. & Demengeot, J. IFN-α/β enhances BCR-dependent B cell responses. *International Immunology* **14**, 411-419, doi:10.1093/intimm/14.4.411 (2002).
91 Soni, C. *et al.* Plasmacytoid Dendritic Cells and Type I Interferon Promote Extrafollicular B Cell Responses to Extracellular Self-DNA. *Immunity* **52**, 1022-1038.e1027, doi:10.1016/j.immuni.2020.04.015 (2020).
92 Bastard, P. *et al.* Autoantibodies against type I IFNs in patients with life-threatening COVID-19. *Science* **370**, eabd4585, doi:10.1126/science.abd4585 (2020).
93 Ehrenfeld, M. *et al.* Covid-19 and autoimmunity. *Autoimmun Rev* **19**, 102597, doi:10.1016/j.autrev.2020.102597 (2020).
94 Gomes, C. *et al.* Autoimmune anti-DNA antibodies predict disease severity in COVID-19 patients. *medRxiv*, 2021.2001.2004.20249054, doi:10.1101/2021.01.04.20249054 (2021).
95 Hansen, C. B. *et al.* SARS-CoV-2 Antibody Responses Are Correlated to Disease Severity in COVID-19 Convalescent Individuals. *J Immunol* **206**, 109-117, doi:10.4049/jimmunol.2000898 (2021).
96 Zuniga, M. *et al.* Autoimmunity to the Lung Protective Phospholipid-Binding Protein Annexin A2 Predicts Mortality Among Hospitalized COVID-19 Patients. *medRxiv*, 2020.2012.2028.20248807, doi:10.1101/2020.12.28.20248807 (2021).
97 Akita, K. *et al.* Interferon α Enhances B Cell Activation Associated With FOXM1 Induction: Potential Novel Therapeutic Strategy for Targeting the Plasmablasts of Systemic Lupus Erythematosus. *Frontiers in Immunology* **11**, doi:10.3389/fimmu.2020.498703 (2021).
98 Rönnblom, L. & Leonard, D. Interferon pathway in SLE: one key to unlocking the mystery of the disease. *Lupus Science & Medicine* **6**, e000270, doi:10.1136/lupus-2018-000270 (2019).
99 Kyogoku, C. *et al.* Cell-specific type I IFN signatures in autoimmunity and viral infection: what makes the difference? *PLoS One* **8**, e83776, doi:10.1371/journal.pone.0083776 (2013).
100 Jeyanathan, M. *et al.* Immunological considerations for COVID-19 vaccine strategies. *Nature Reviews Immunology* **20**, 615-632, doi:10.1038/s41577-020-00434-6 (2020).
101 Oja, A. E. *et al.* Divergent SARS-CoV-2-specific T- and B-cell responses in severe but not mild COVID-19 patients. *Eur J Immunol* **50**, 1998-2012, doi:10.1002/eji.202048908 (2020).

102 Sauer, K. & Harris, T. An Effective COVID-19 Vaccine Needs to Engage T Cells. *Front Immunol* **11**, 581807, doi:10.3389/fimmu.2020.581807 (2020).
103 Hu, J. *et al.* Emerging SARS-CoV-2 variants reduce neutralization sensitivity to convalescent sera and monoclonal antibodies. *Cellular & Molecular Immunology* **18**, 1061-1063, doi:10.1038/s41423-021-00648-1 (2021).
104 Redd, A. D. *et al.* CD8+ T cell responses in COVID-19 convalescent individuals target conserved epitopes from multiple prominent SARS-CoV-2 circulating variants. *Open Forum Infectious Diseases*, doi:10.1093/ofid/ofab143 (2021).
105 Gustine, J. N. & Jones, D. Immunopathology of Hyperinflammation in COVID-19. *Am J Pathol* **191**, 4-17, doi:10.1016/j.ajpath.2020.08.009 (2021).
106 Zheng, H. *et al.* Multi-cohort analysis of host immune response identifies conserved protective and detrimental modules associated with severity across viruses. *Immunity*, doi:10.1016/j.immuni.2021.03.002.
107 van Eeden, C., Khan, L., Osman, M. S. & Cohen Tervaert, J. W. Natural Killer Cell Dysfunction and Its Role in COVID-19. *Int J Mol Sci* **21**, doi:10.3390/ijms21176351 (2020).
108 Stoeckius, M. *et al.* Cell Hashing with barcoded antibodies enables multiplexing and doublet detection for single cell genomics. *Genome Biol* **19**, 224, doi:10.1186/s13059-018-1603-1 (2018).
109 Bray, N. L., Pimentel, H., Melsted, P. & Pachter, L. Near-optimal probabilistic RNA-seq quantification. *Nature Biotechnology* **34**, 525-527, doi:10.1038/nbt.3519 (2016).
110 Melsted, P. *et al.* Modular, efficient and constant-memory single-cell RNA-seq preprocessing. *Nature Biotechnology*, doi:10.1038/s41587-021-00870-2 (2021).
111 Stuart, T. *et al.* Comprehensive Integration of Single-Cell Data. *Cell* **177**, 1888-1902 e1821, doi:10.1016/j.cell.2019.05.031 (2019).
112 R Core Team. R: A Language and Environment for Statistical Computing. (R Foundation for Statistical Computing, Vienna, Austria, 2018).
113 Gayoso, A. *et al.* Joint probabilistic modeling of single-cell multi-omic data with totalVI. *Nature Methods* **18**, 272-282, doi:10.1038/s41592-020-01050-x (2021).
114 Hänzelmann, S., Castelo, R. & Guinney, J. GSVA: gene set variation analysis for microarray and RNA-Seq data. *BMC Bioinformatics* **14**, 7, doi:10.1186/1471-2105-14-7 (2013).
115 Liberzon, A. *et al.* The Molecular Signatures Database (MSigDB) hallmark gene set collection. *Cell Syst* **1**, 417-425, doi:10.1016/j.cels.2015.12.004 (2015).

Schematic 1

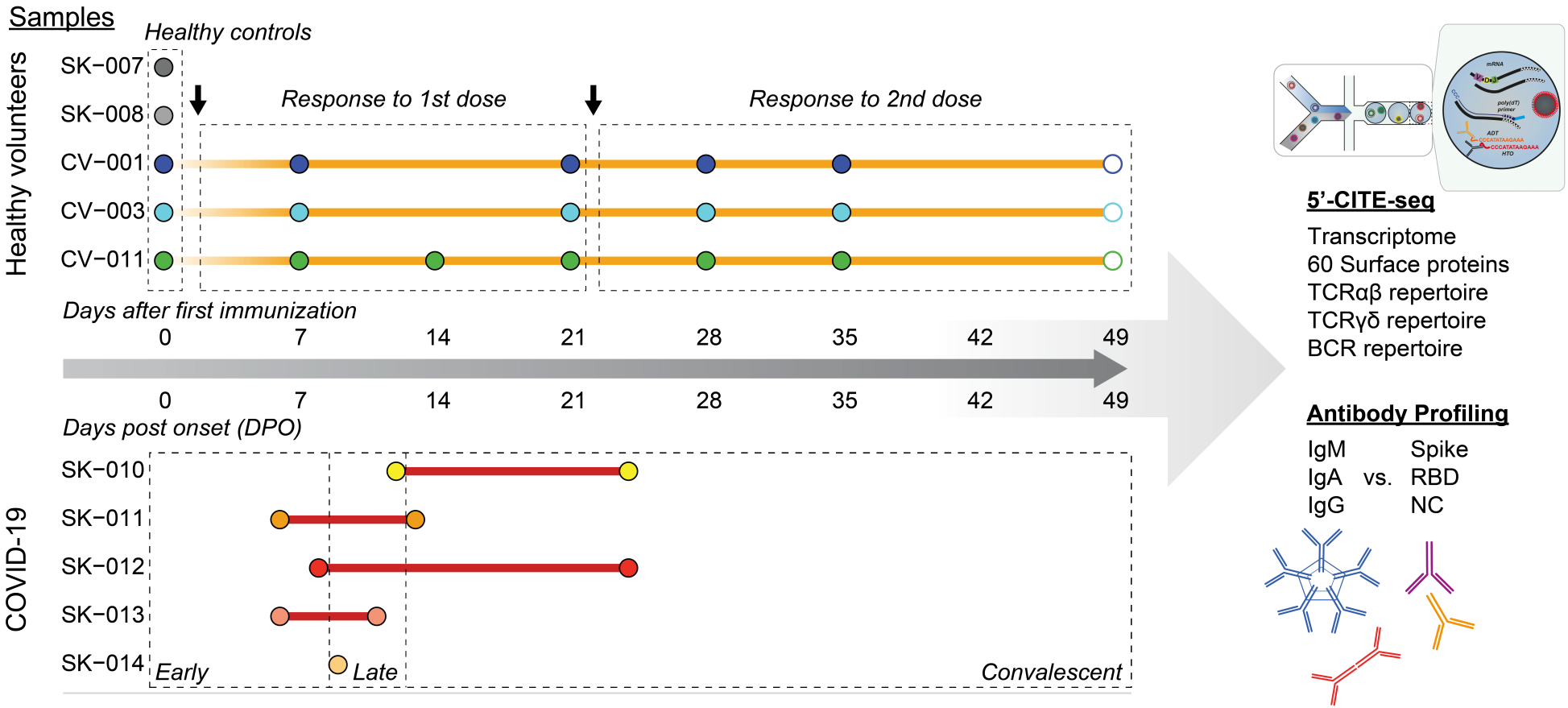

Fig. 1

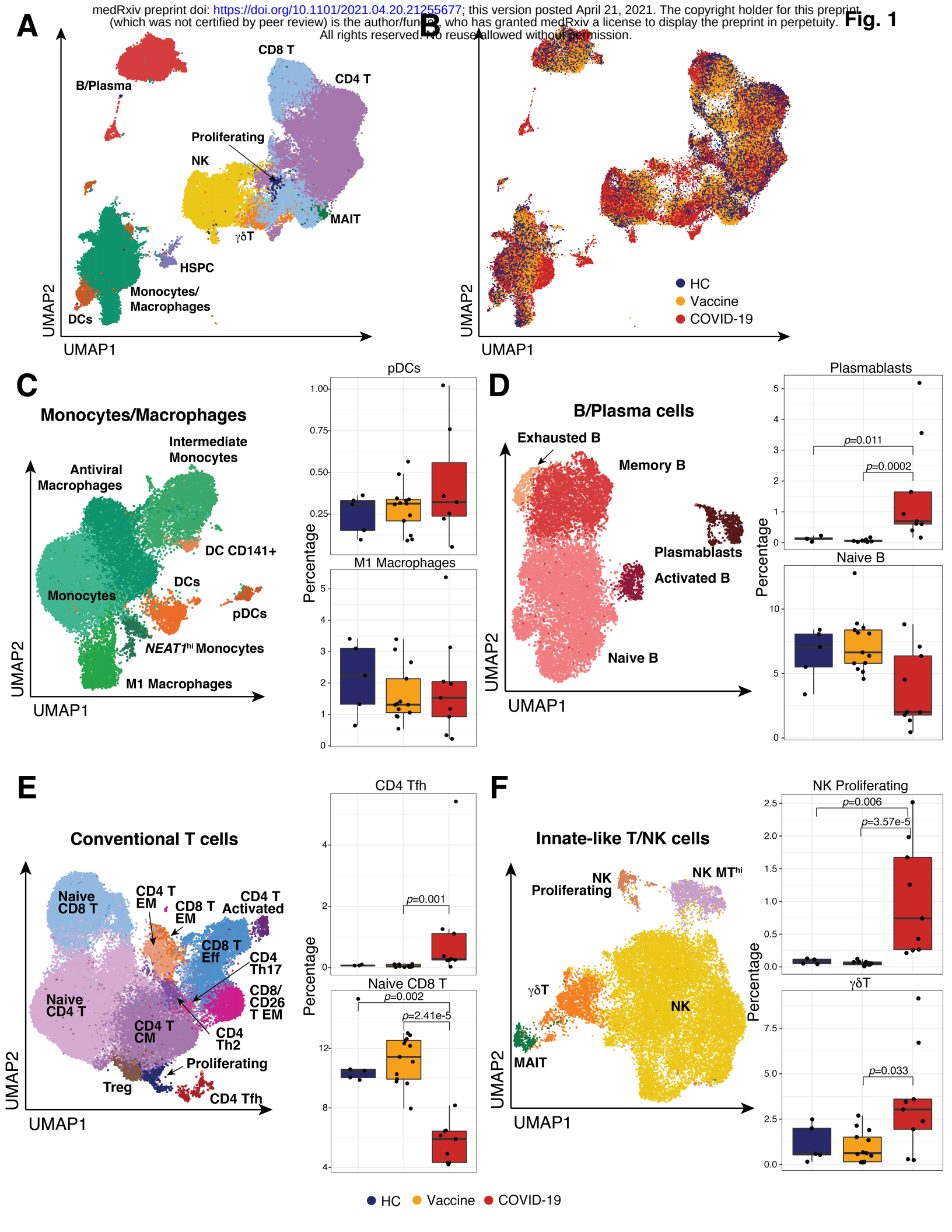

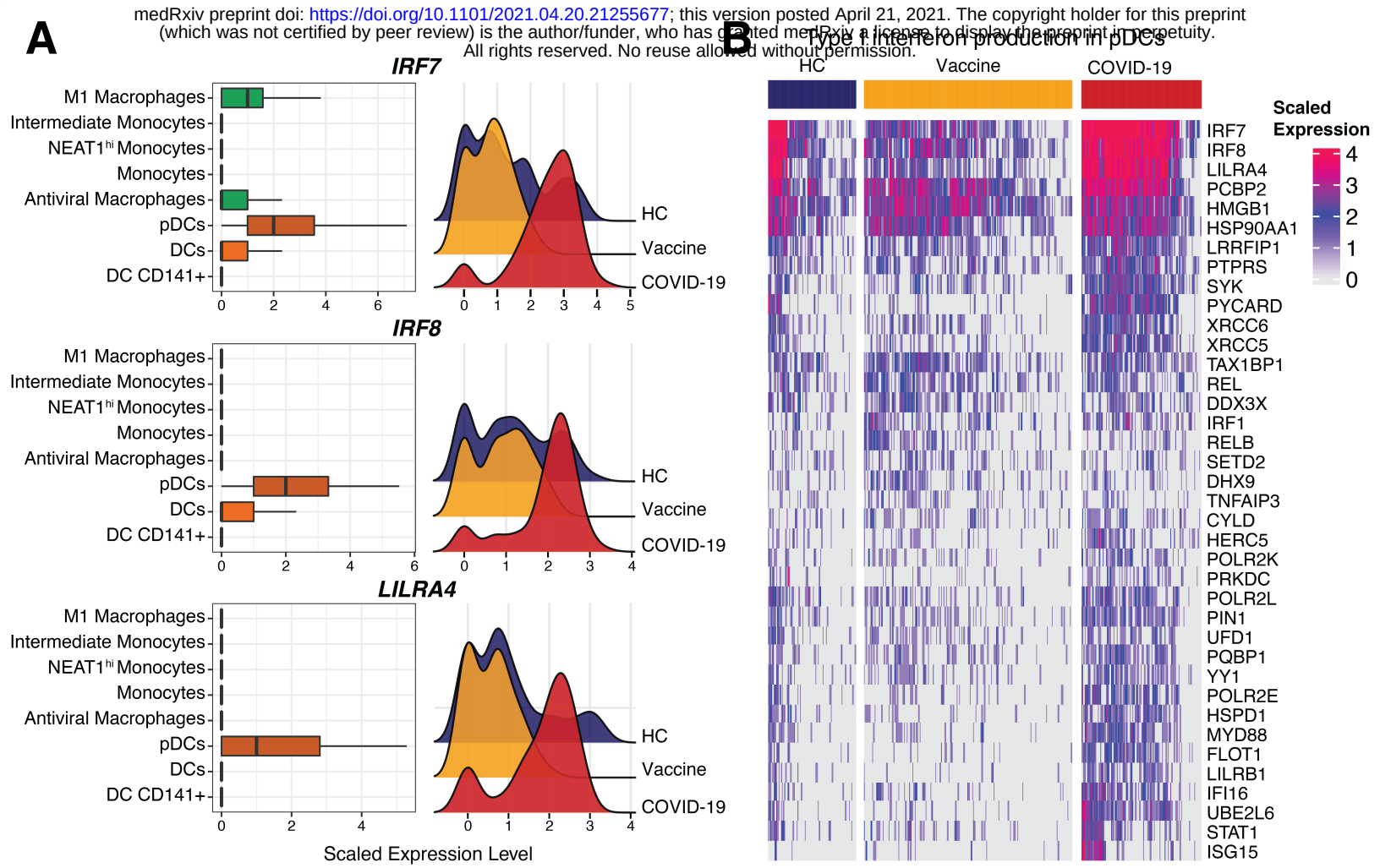

Fig. 2

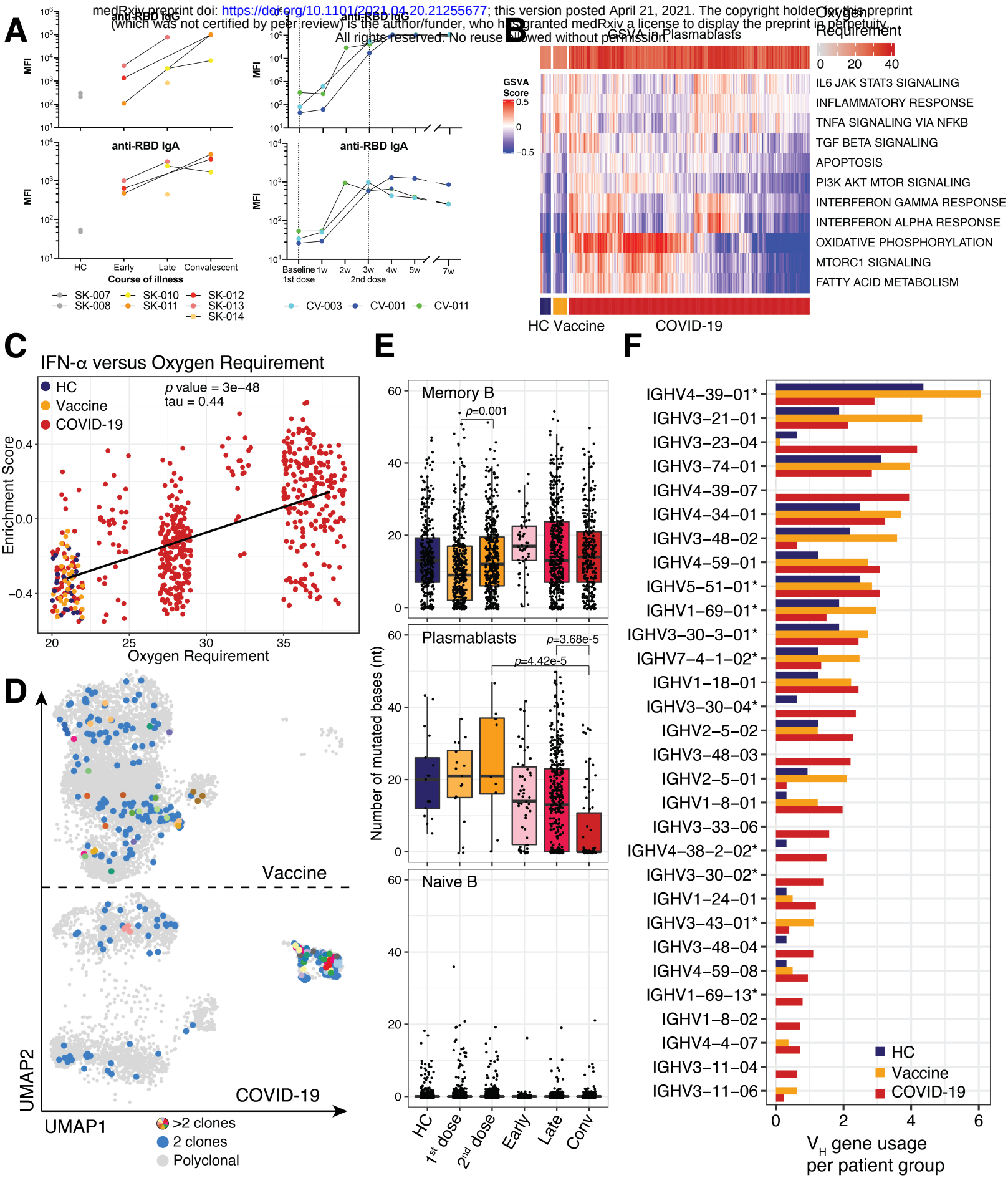

Fig. 3

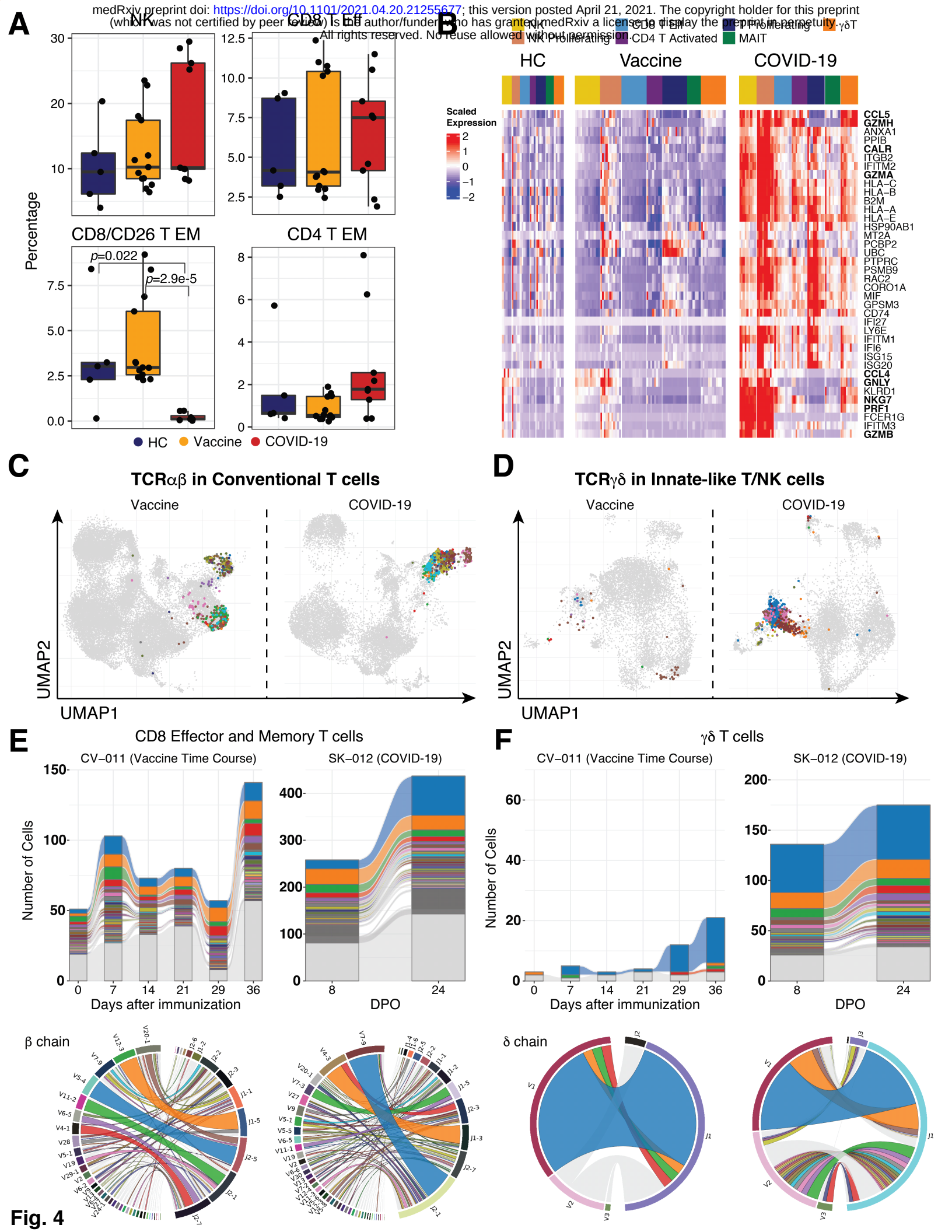

Fig. 4

Supplemental Figure Legends

Supplemental Figure 1: Analysis of immune landscape in COVID-19 and in vaccinated individuals

- **a.** Distribution of signal from characteristic ADTs. UMAP representation of all immune subsets can be found in Fig. 1A.
- **b.** Boxplots of major immune subsets from PBMCs of COVID-19 patients, healthy individuals immunized with BNT162b2 and un-immunized healthy volunteers. P-values are determined by a Wilcox test.

Supplemental Figure 2: Detailed analysis of immune subsets

Boxplots showing innate (**a**)**,** B cell (**b**), T cells (**c**) and innate-like lymphocytes (**d**) proportions in the COVID-19 patient, vaccinated individuals and un-immunized HC PBMCs. P-values are determined by a Wilcox test.

Supplemental Figure 3: Expression of type I interferon pathway in M1 Macrophages

- **a.** Expression of *IRF7*, *IRF8*, and *LILRB1* in M1 macrophages from HC, Vaccine samples and COVID-19 patients.
- **b.** Scaled and normalized expression of IFN production-associated genes in M1 macrophages based on gene ontology (GO) gene set for type I IFN production (GO:0032606).

Supplemental Figure 4: Ab titers and plasmablast responses

SARS-CoV-2-specific Ab titers were assessed for COVID-19 patients and healthy volunteers using a Multiplex Bead Binding Assay (MBBA). IgG, IgA and IgM anti-NC responses are shown in (**a**), anti-spike responses in (**b**). IgM responses to RBD are shown in (**c**), with IgA and IgG anti-RBD responses shown in Fig. 3.
Per sample PCA plot based on combined gene sets for IFN response and IFN stimulated gene signatures is shown in (**d**), with the expression of four transcripts with strong correlations to PC1 indicated above.

Supplemental Figure 5: Tfh response signature

GSVA of Tfh responses in COVID-19 patient biospecimens and in cells from healthy volunteers.

Supplemental Figure 6: Assessment of clonal T cell responses

a and b. Evaluation of clonal responses in CD8 T eff population from COVID-19 patients (**a)** and HCs (**b**), with bar graphs showing clonal repertoire distribution among CD8 T_{EM} and T_{eff} cells based on TCRβ CDR3 sequences. Polyclonal cells in grey. Circos plots of frequencies of Vβ and Jβ usage are shown (bottom).

c and d. Clonal repertoire distribution among γδ T cells based on TCRδ CDR3 sequence in COVID-19 patients (**a)** and HCs (**b**). Polyclonal cells in grey. Circos plots of frequencies of Vδ and Jδ usage are shown (bottom).

Supplemental Table 1

Participant	Cohort	Age	Sex	Days post onset symptoms or days since first vaccine dose	Fraction inspired O_2	WHO COVID severity scale	COVID Outcome
SK-010	Acute COVID-19	35-40	Female	12	21	5	Recovered
				24	21		
SK-011	Acute COVID-19	55-60	Female	6	32	7	Recovered
				13	24		
SK-012	Acute COVID-19	45-50	Male	8	38	8	Recovered
				24	38		
SK-013	Acute COVID-19	60-65	Male	6	38	5	Recovered
				11	28		
SK-014	Acute COVID-19	55-60	Female	9	36	5	Recovered
SK-007	Healthy	35-40	Female	NA	21	NA	NA
SK-008	Healthy	35-40	Male	NA	21	NA	NA
CV-001	mRNA vaccine	35-40	Male	0, 7, 21, 28, 35, 54	21	NA	NA
CV-003	mRNA vaccine	30-35	Male	0, 10, 20, 28, 35, 52	21	NA	NA
CV-011	mRNA vaccine	35-40	Male	0, 7, 14, 21, 29, 36, 50	21	NA	NA

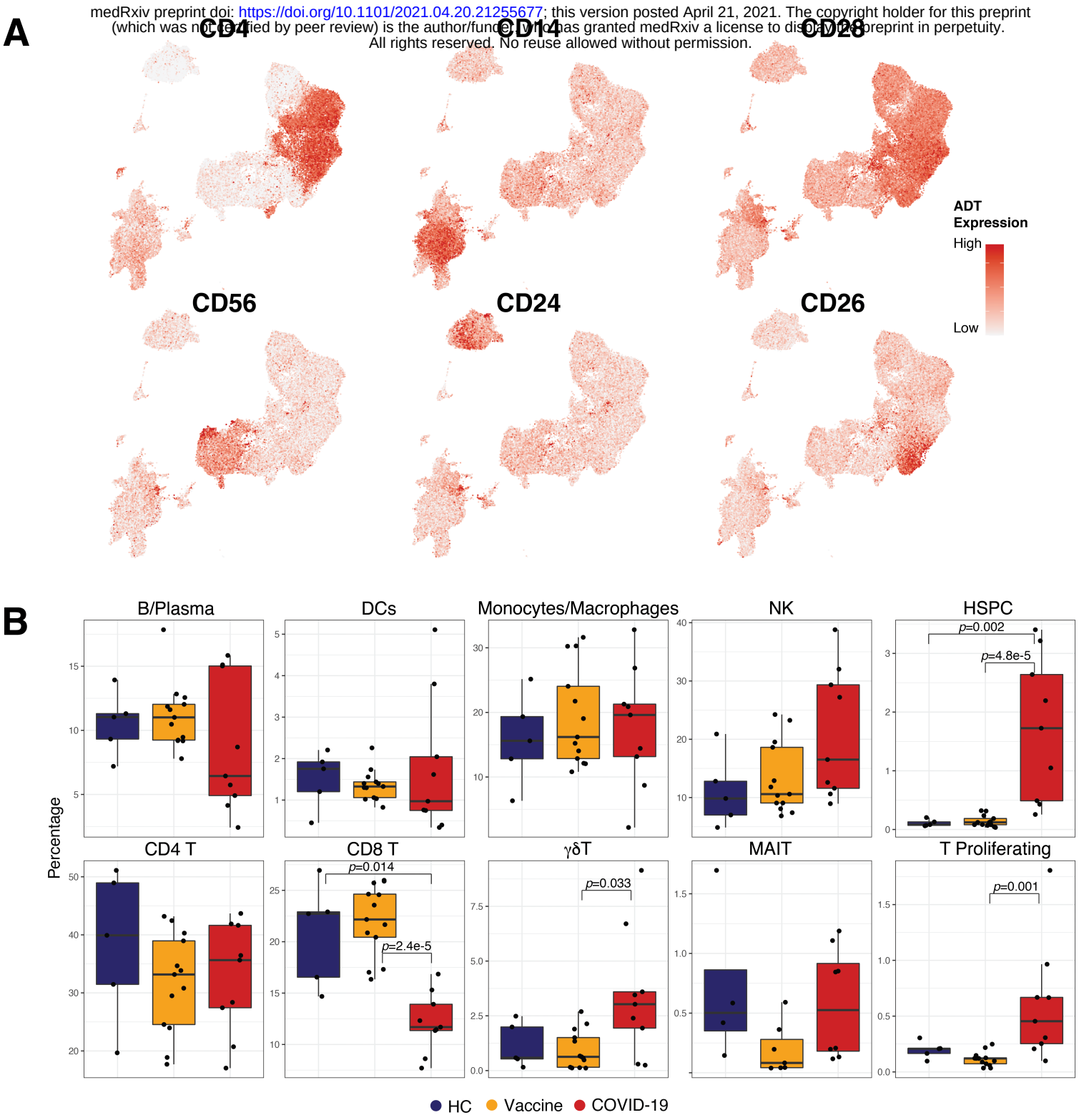

Supplemental Fig. 1

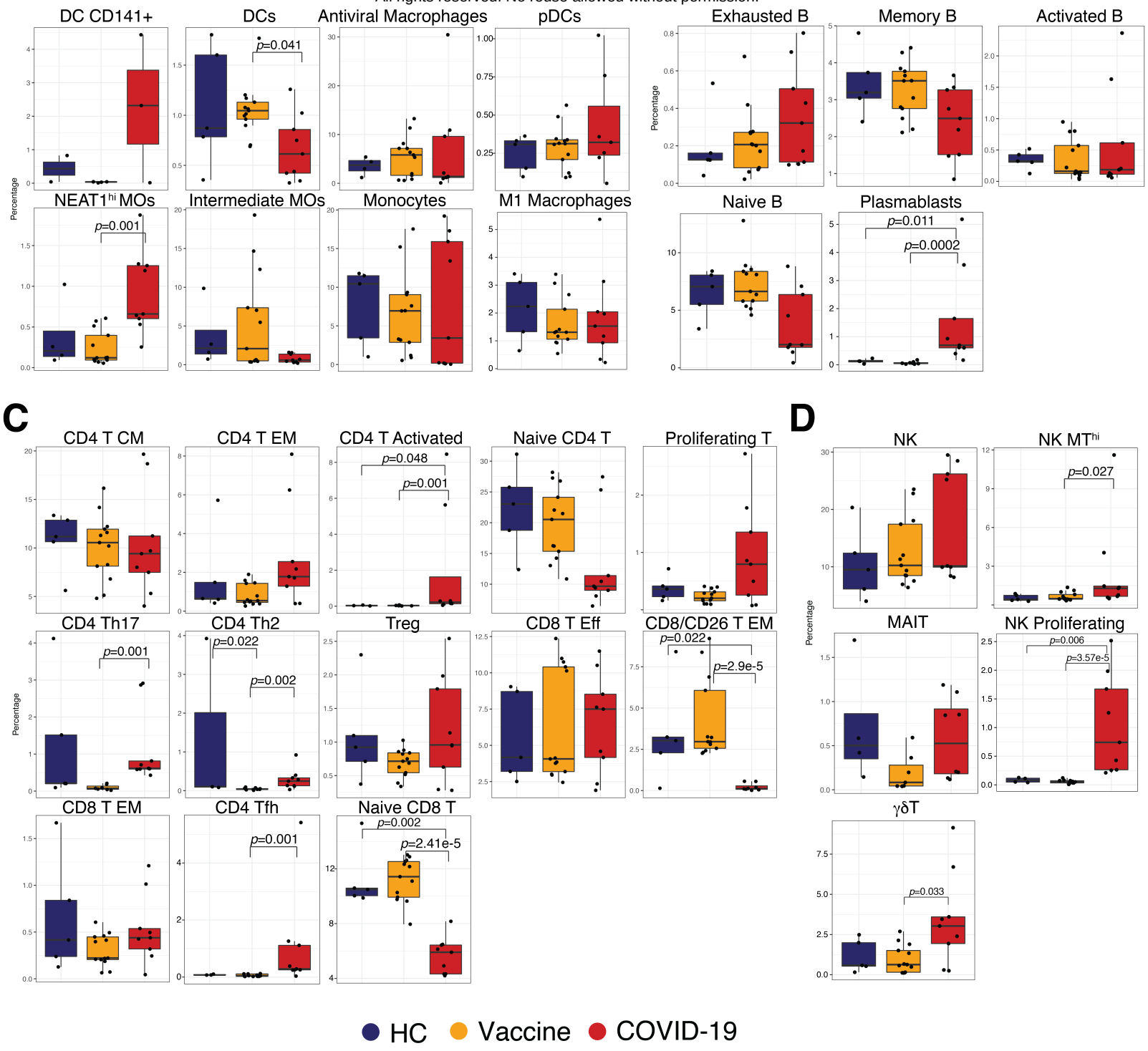

Supplemental Fig. 2

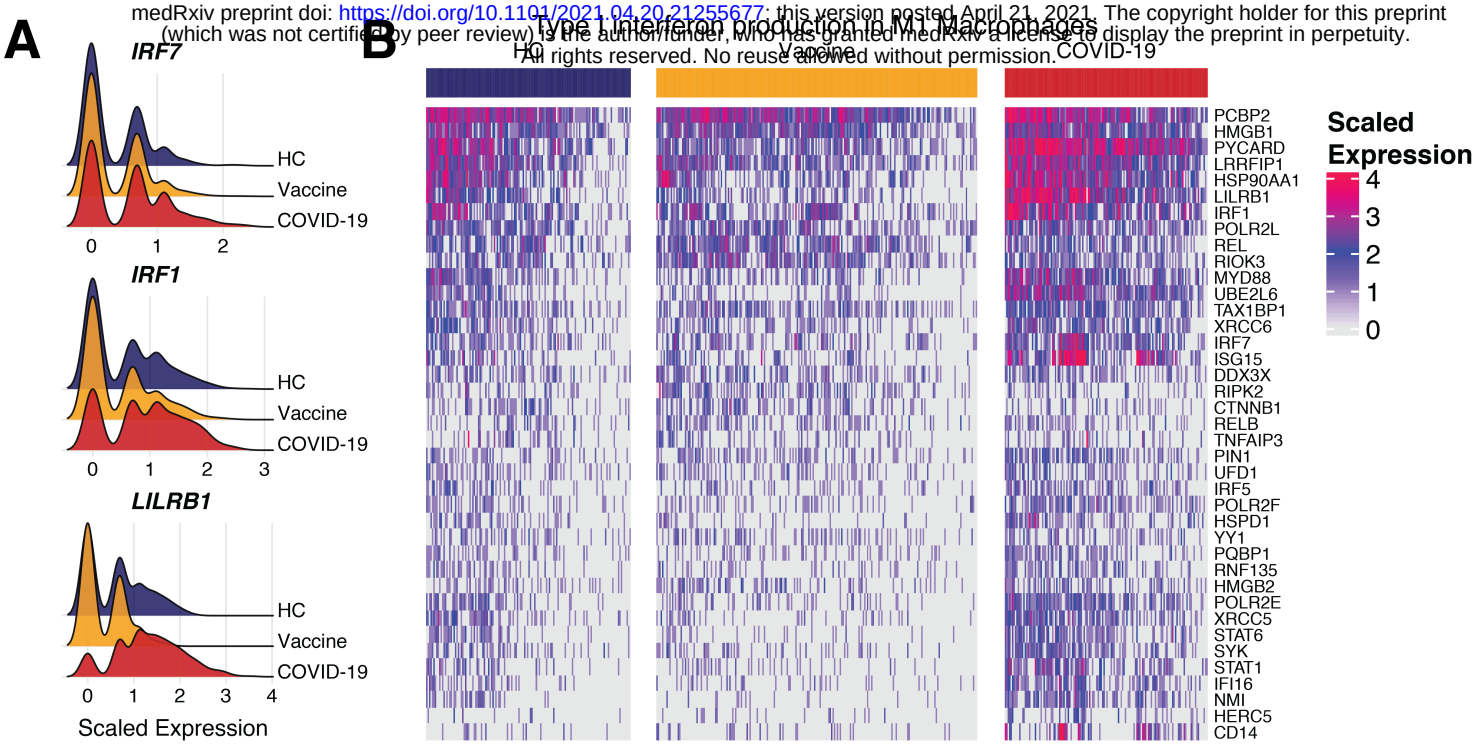

Supplemental Fig. 3

A

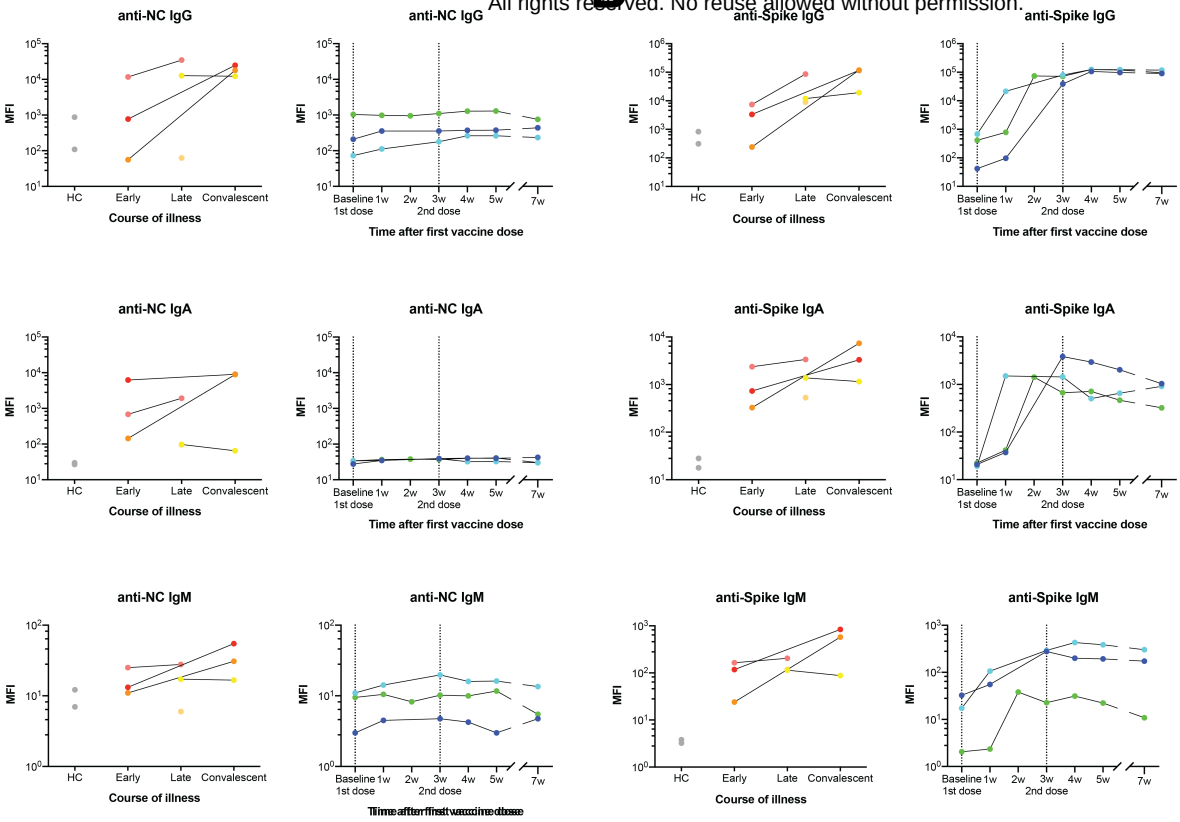

B

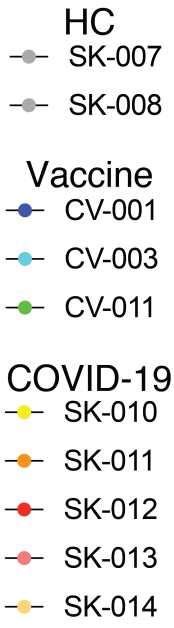

C

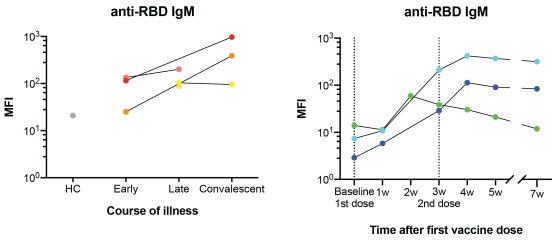

D

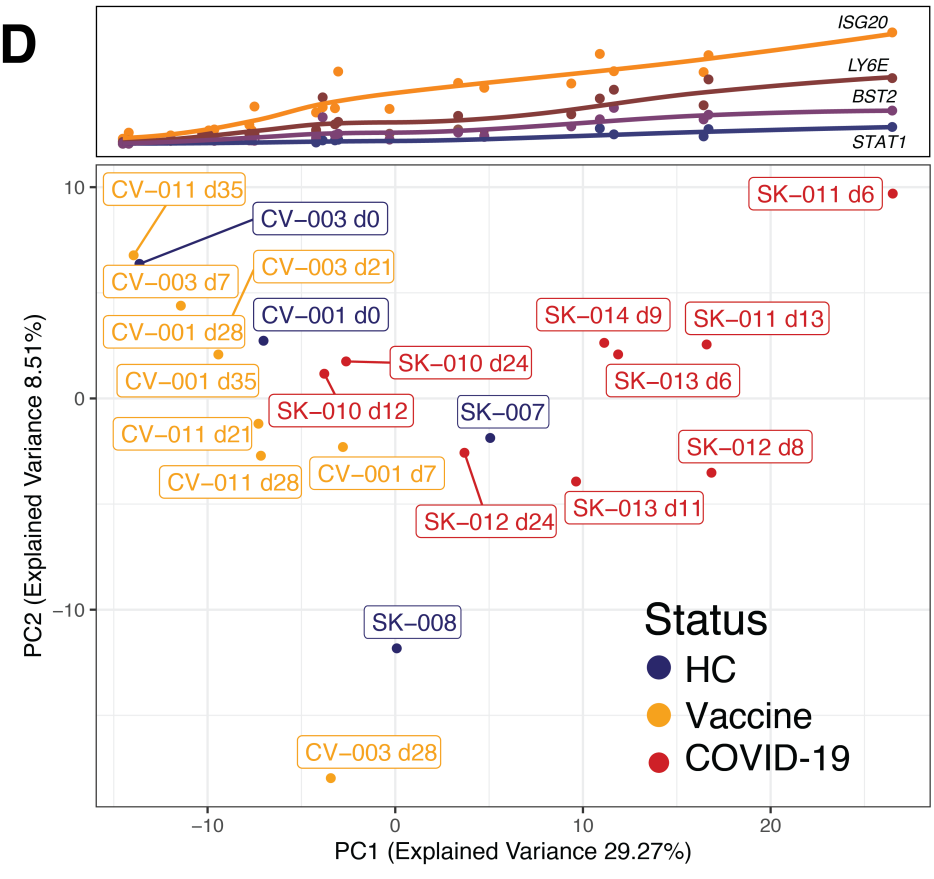

Supplemental Fig. 5

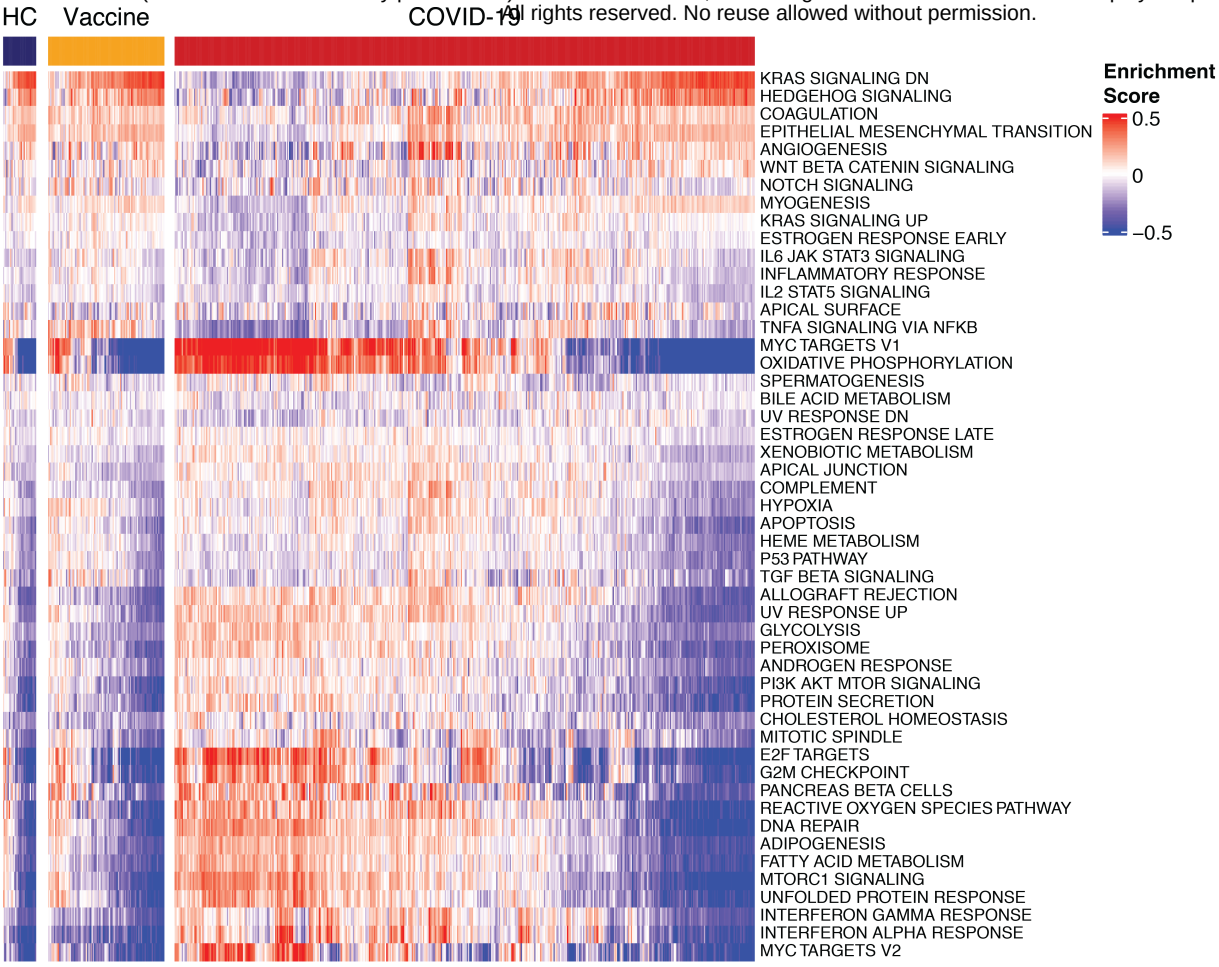

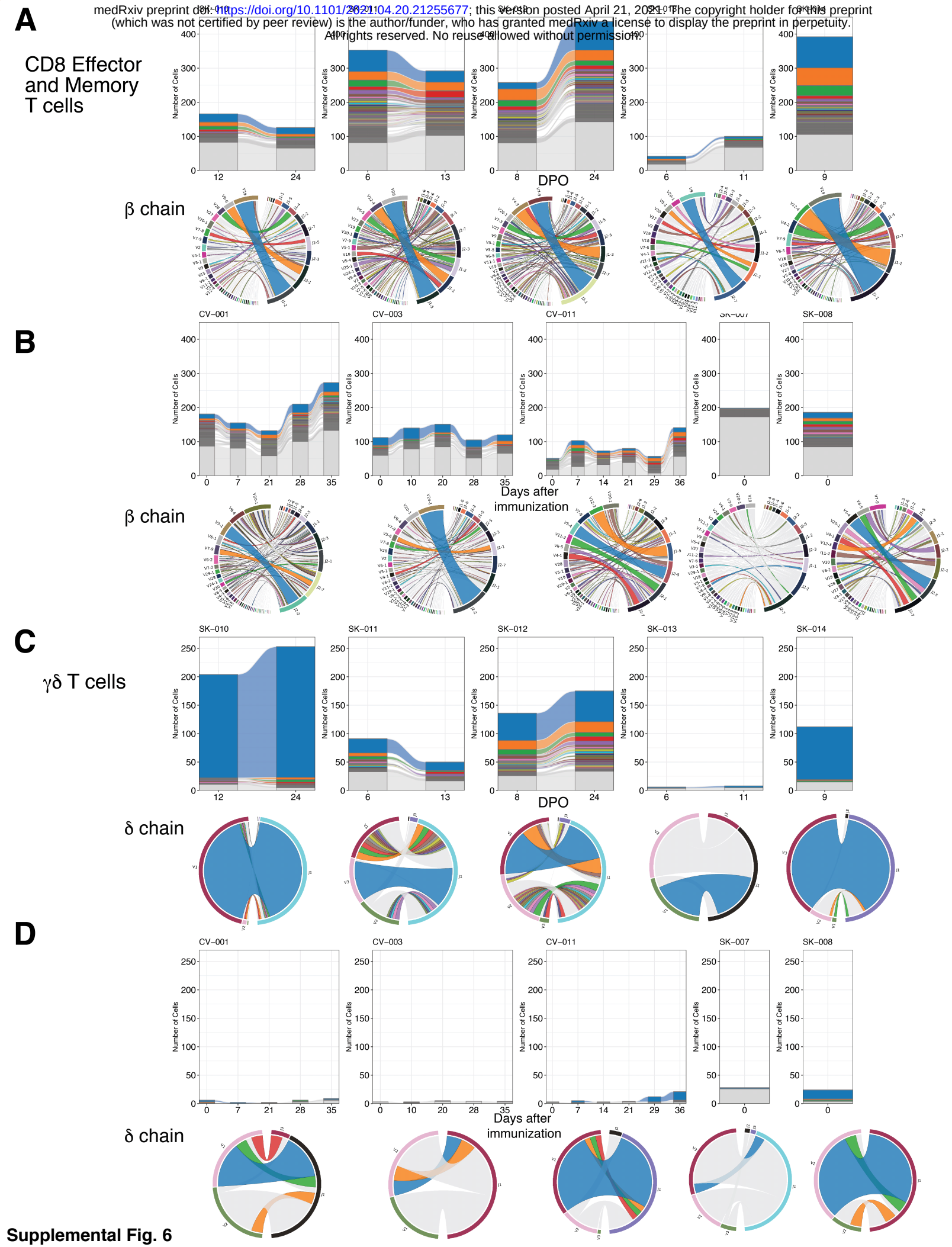

Supplemental Fig. 6